Subsurface Geology and Geothermal Potential of the Kavaklıdere Geothermal Field (Western Turkey)

Ozdemir, A.[1], Sahinoglu, A.[2]

[1]Adil Ozdemir Engineering and Consulting, Öveçler Mah. 1322 Sok. 60/5 Çankaya, Ankara, Turkey

[2]Istanbul Rumeli University, Graduate School of Natural and Applied Science, Istanbul, Turkey

Abstract: ***The Kavaklıdere geothermal field which covers a 126 km^2 area between Alaşehir and Salihli districts in Manisa province, Turkey were studied. The various parameters connected to geological structure and the properties of geothermal systemsin the field were measured.The important methods which are various electrical resistivity and thermal methods in geothermal exploration were applied in the field and also containing of geothermal fluids were usually characterized by low resistivity. VES applications AB/2 = 2500 m theoretical depth in 206 locationswereapplied. Measuring point range was taken between 250 m and 500 m. In addition to total 206 resistivity measurements were compared with previous studies and all measurements were re-evaluated with EarthImager 1D and RockWorks programs. VES curves, resistivity and stratigraphy cross-sections were re-prepared and re-interpreted. At the result of the those measurements, potential geothermal reservoirs were detected for determining the expected thermal activities at intersection points of the different orientioned faults mostly located at middle and north sides of the study area.***

Keywords: Western Anatolia, Geothermal Research, High Temperature Geothermal Field, Electiric Resistivity, Conceptual Modelling

1. Introduction

Geothermal energy comes from the natural heat of the Earth. The energy is an efficient heating and cooling alternative for residential, commercial, and lectirical power generation and industrial applications. 1,200 thermomineral springs due to the geological structure resulting from young tectonic and volcanic activities have been appeared in Turkey. Especially in the western part of Turkey, the conditions are excellent due to the presence of horst and graben structures. The initial studies at Salihli-Alaşehir districts located in the western section of Gediz Graben in Western Anatolia have begun in 1960's because of many high-temperature geothermal resources located in region. The Kavaklıdere geothermal field is located in the Gediz Graben one of the important Western Anatolia graben structures. In addition, geological mapping, geophysical surveys and exploration drilling of studied field of 126 km^2 area in the Alaşehir district (Manisa), were carried out in the geothermal fields of the Gediz Graben by MTA (General Directorate of Mineral Research and Exploration of Turkey) (Fig. 1 and 2).

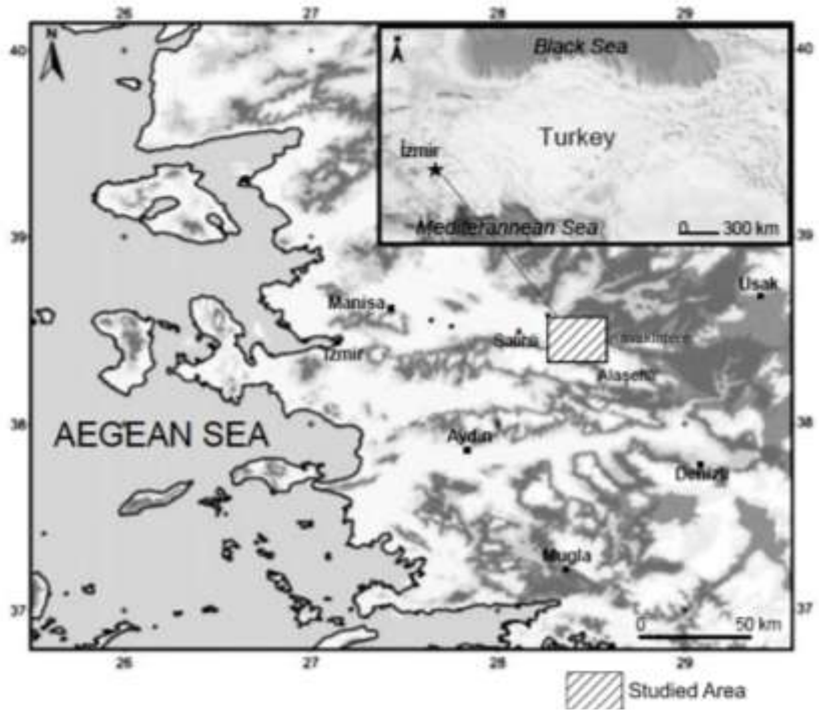

Figure 1: Location map of the Kavaklıdere geothermal field

The stratigraphy, petrography, and tectonics of the the field area have been extensively studied (Emre, 1996; Seyitoglu et al., 2000), geological and petroleum survey (Yılmazer et al., 2010;Yazman and Iztan, 1990; Ünal and Havur, 1971); geothermal exploration (Özdemir et al., 2017; Özdemir, 2015) and gravity and magnetic (MTA, 2010); seismic and gravity survey (Yazman et al., 1998; Gürsoy, 1981; Türk, 2014);geological structure, stratigraphy and tectonic characteristics (MTA, 2011a); hydrothermal alteration studies, geological, hydrogeological and water chemistry evaluations (MTA, 2011b and Şimşek, 2012); the chemical analyses of hot and cold water samples (MTA, 2011c); structure and tectonics of the Alaşehir detachment fault and supra-detachment basin (Öner, 2012 and active tectonic (Koçyiğit, 2014). Six different units were distinguished in the survey area which constitutes the Kavaklıdere geothermal field. These six units from bottom to top were (1) Metamorphic rocks (gneiss, calc-schist, quartz-schist, phyllite, mica-schist) of the Precambrian-Middle Triassic Menderes Massif (2) Paleozoic marbles (3) Granitic rocks (4) Upper Miocene-Lower Pliocene Gediz formation (5) Upper Pliocene-Quaternary sediments and Kaletepe formation (6) Quaternary alluviums, respectively (Özdemir et al., 2017) (Fig. 3). Graben of the study area developed in the control of the structure and lithology. Folds, faults, joint systems and lithologic properties have been effective in morphology. From the Miocene to the present, plains of erosion have seen at several levels. Recent studies suggest that the main faults of the graben are normal faults and cut the detachment fault separating the Menderes Massif rocks from the Neogene terrestrial sediments. Graben faults intersect the Upper Miocene unit conglomerates and sandstones outcropping at the edges of the graben, Pliocene units consisting of detritic sandstones and claystones and Quaternary sediments. The depression basin bordered by normal faults from the edges is a graben, and it is named the Gediz Graben. This graben structure is especially apparent in this basin which ends by narrowing at the eastern edge, but the morphologic borders of the western part of it are difficult to draw. The fault planes are typically flat and no folding has developed at the sediments between the fault blocks. On the other hand, the topographic surfaces of the descending blocks slope towards the ascending blocks. It is known that the basement of graben subsided by a minimum of 1500 m after the Pliocene. This value accounts for 1 mm subsidence per year (Özdemir et al., 2017). Metamorphics that constitute the highlands surrounding the graben from the south and north consist of gneiss, marbles, quartzites and schists. Some of the faults bordering the graben formed contacts between the metamorphic base rocks and Miocene, Pliocene and Quaternary sediments.

Figure 2: Generalised structural geology of the Kavaklıdere geothermal field (revised from Öner and Dilek,2011)

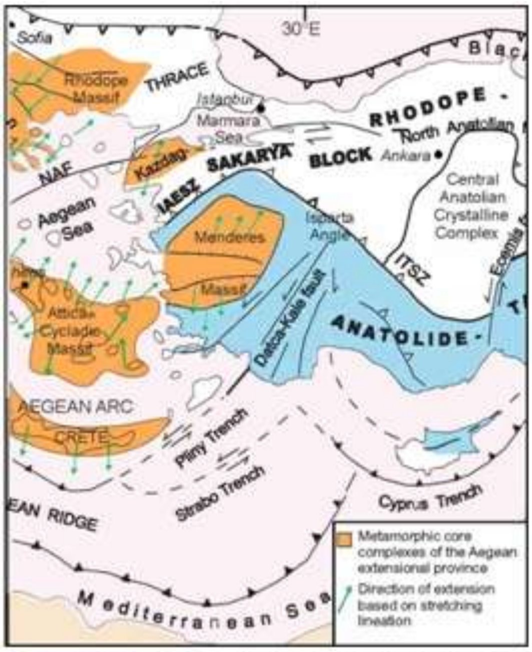

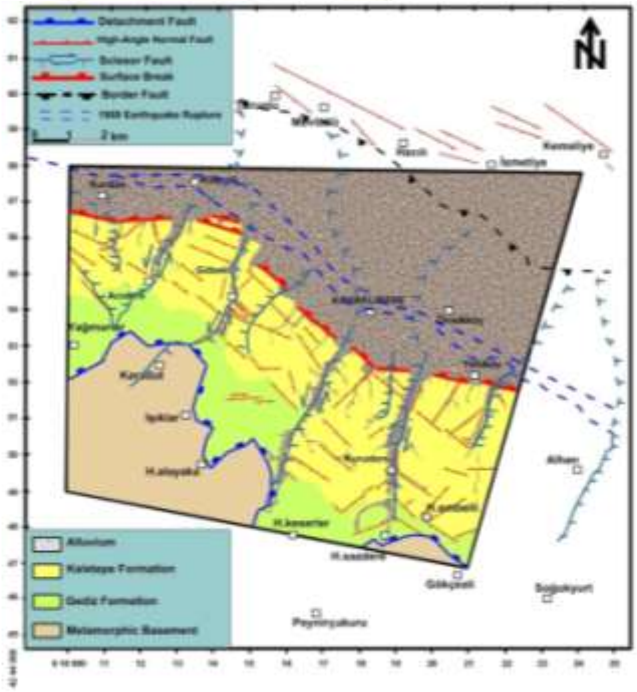

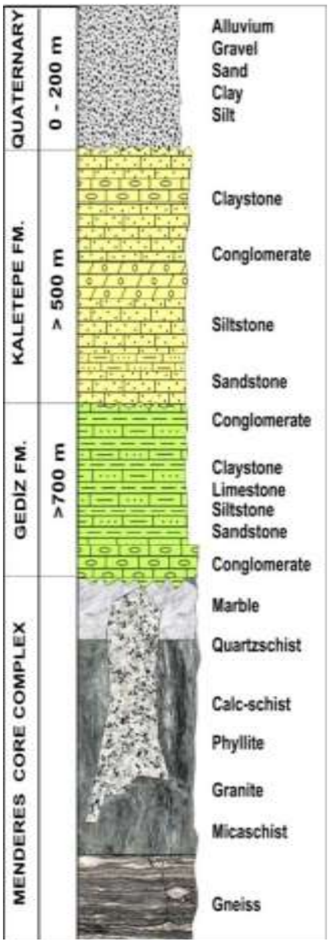

Figure 3: Simplified geological map and generalized stratigraphic vertical section of the Kavaklıdere geothermal field (Özdemir et al., 2016)

"Report on Kavaklıdere Field Resistivity Survey" (Özdemir, 2015) in the Kavaklıdere geothermal field was prepared and VES measurements were measured.In addition to the measurements made in the scope of the this study, total 206 resistivity measurements measured during previous studies were re-evaluated with EarthImager 1D and RockWorks programs. VES curves, resistivity and stratigraphy cross-sections were re-prepared and re-interpreted. At the result of the those measurements, potential geothermal reservoirs were detected for determining the expected thermal activities at intersection points of the different orientioned faults mostly located at middle and north sides of the study area.

The aim of this study is to discuss the geological properties and the geothermal characteristics of the The Kavaklıdere geothermal field. Geological materials are generally poor electrical conductors and have a high resistivity. Geothermal fluids in the pores and fractures of the earth, however, increase the conductivity of the subsurface material. This change in conductivity is used to map the subsurface geology and estimate the subsurface material composition. Therefore, those methods which measure the electrical resistivity at depth in the ground have been the most useful of all geophysical methods used to prospect for geothermal reservoirs.

2. Geophysical Exploration

Geophysical methods can often provide information as effectively, and certainly at a lower cost, than drilling a borehole. It should be recognized that no particular technique is universally applicable, and methods should be chosen carefully to suit the situation. Most geophysical methods display a progressive reduction of resolving capacity as they are extended to greater depths. The effectiveness of these geophysical methods was greatly increased when emphasis was shifted from prospecting the geology and the structures that contain the geothermal fluids to prospecting the fluids themselves and concentrating on determining those parameters which are most sensitive to changes in temperature. The various parameters connected to geological structure and the properties of geothermal systems weremeasured. In geothermal exploration the task is the detection and delineation of geothermal resources, the location of exploitable reservoirs and the siting of drillholes through which hot fluids at depth was extracted. In geothermal exploration, the important methods were various electrical and thermal methods. Rocks containing geothermal fluids were usually characterized by anomalously low resistivity. Therefore, those methods which measure the electrical resistivity at depth in the ground were the most useful of all geophysical methods used to prospect for geothermal reservoirs. Further, it should be born in mind that geophysical exploration cannot stand alone, but must be applied along with field geology, geochemistry and drilling in order to resolve the nature of the subsurface geothermal systems in as much detail as possible (Hersir and Bjornsson, 1991).

2.1. Electrical resistivity (Vertical electrical soundaing / VES) method

Measuring the electrical resistivity of the subsurface is the most powerful prospecting method in geothermal exploration. Resistivity is directly related to the properties of interest, like salinity, temperature, alteration and porosity (permeability). To a great extent, these parameters characterize the reservoir. The most important factors are the porosity, temperature, salinity and the water-rock interaction. In geothermal areas, the rocks are water-saturated. Ionic conduction in the saturating fluid depends on the number and mobüity of ions and the connectivity of flowpaths through the rock matrix. Usually, the saturating fluid is among the dominant conductor in the rock and the degree of saturation is of great importance to the bulk resistivity. The pressure dependence is negligible compared to the temperature dependence, provided that the pressure is sufficiently high so that there is no change in phase. The bigger the mean fracture width of the pores is, the bigger is the fracture porosity. There-fore, in most cases, high fracture porosity is followed by high permeability. This close relationship between porosity and, hence, electrical resistivity, on the one hand and permeability on the other hand, has great importance in electrical exploration of potential geothermal areas. That is, for intergranular porosity, high permeability may accompany low resistivity.An electrical method is either a sounding method or a profiling method,depending on what kind of a resistivity structure is being investigated. The sounding method is used for mapping resistivity as a function of depth. The profiling method maps resistivity at more or less constant depth and is used to map lateral resistivity changes (Hersir and Bjornsson, 1991).

Vertical electrical sounding (VES)is a geophysical method for investigation of a geological medium. The method is based on the estimation of the electrical conductivity or resistivity of the medium. The estimation is performed based on the measurement of voltage of electrical field induced by the distant grounded electrodes (current electrodes). In the Schlumberger array two potential and two current electrodes are placed along a straight line.

2.2. Electrical resistivity (VES) measurements

Electrical resistivity method were applied for the geothermal exploration in study area. Electrical resistivity method was made Schlumberger electrode array. Lateral interactions decreases and active penetration depth increases in this array where the gradient value of potential function is measured. Especially this method is used for deep surveys.

Electirical resistivity (VES) applications by a private company made in the Kavaklıdere geothermal field was aimed to develop the field and research the geothermal energy possibilities in the field. Detecting structure of the undergroung and active tectonism by understanding geology in covered areas were evaluated within the extent of purposes.

There are some other wells drilled previously and in some of these wells high temperatures were reached. Also fluids with various flow speeds and high temperatures were found in drilled wells. "Report on Kavaklıdere Field Resistivity Survey" (Özdemir, 2015) in the Kavaklıdere geothermal field was prepared. VES measurements were measured by a private company.In addition to the measurements made in the scope of the this study, total 206 resistivity measurements measured during previous studies re-evaluated with EarthImager 1D and RockWorks programs. VES curves, resistivity and stratigraphy cross-sections is re-prepared and re-interpreted by authors.

Resistivity applications were executed along Sclumberger electrode array by making Vertical Electric Sounding (VES). VES measurements were made in 206 locations (Table 1). VES measurement locations were given in Fig. 4. In VES applications AB/2 = 2500 m theoretical depth has been researched. Measuring point range varies between 250 m and 500 m.

Table 1: Coordinates of measurement points of vertical electrical sounding (VES) (UTM -ED50)

VES No	*Y*	*X*	*Z (m)*	*VES No*	*Y*	*X*	*Z (m)*
DES-1	622981	4257504	155	**DES-44**	620000	4253000	186
DES-2	623495	4257497	161	**DES-45**	622050	4255075	128
DES-3	622500	4258000	159	**DES-46**	621000	4255400	130
DES-4	621960	4257975	146	**DES-47**	621045	4256000	126
DES-5	623000	4258000	160	**DES-48**	616000	4257000	128
DES-6	623500	4258000	170	**DES-49**	615030	4257050	135
DES-7	623910	4258000	180	**DES-50**	623000	4254600	130
DES-8	622500	4257500	150	**DES-51**	622480	4255020	130
DES-9	622000	4257500	145	**DES-52**	620520	4256020	125
DES-10	623510	4256510	129	**DES-53**	621525	4255600	126
DES-11	623500	4257000	149	**DES-54**	621000	4256500	130
DES-12	623000	4256500	130	**DES-55**	621500	4256000	125
DES-13	623000	4257000	141	**DES-56**	619500	4256500	129
DES-14	622550	4257050	146	**DES-57**	621556	4257905	142
DES-15	622500	4256500	129	**DES-58**	620500	4258000	162
DES-16	621515	4257500	137	**DES-59**	620508	4257578	135
DES-17	622000	4257000	132	**DES-60**	620500	4257000	124
DES-18	621000	4258000	146	**DES-61**	620018	4257565	128
DES-19	621000	4257175	130	**DES-62**	619500	4257500	128
DES-20	621000	4257550	138	**DES-63**	618500	4257500	123
DES-21	620000	4257964	126	**DES-64**	621500	4257000	128
DES-22	620000	4257088	125	**DES-65**	621500	4256500	126
DES-23	619986	4255986	127	**DES-66**	622000	4256500	125
DES-24	618950	4257940	120	**DES-67**	622000	4256000	126
DES-25	618000	4258000	116	**DES-68**	623000	4256000	130
DES-26	617000	4258000	119	**DES-69**	622500	4255500	122
DES-27	614421	4256983	138	**DES-70**	623000	4255500	128
DES-28	618950	4257000	125	**DES-71**	617530	4256491	132
DES-29	618000	4257000	124	**DES-72**	618500	4256500	128
DES-30	622000	4255500	125	**DES-73**	618500	4255500	131
DES-31	622550	4254600	130	**DES-74**	619500	4255500	130
DES-32	623000	4255000	125	**DES-75**	618500	4258000	118
DES-33	623500	4256000	130	**DES-76**	620000	4256500	123
DES-34	622500	4255955	125	**DES-77**	620000	4255500	133
DES-35	622525	4253500	126	**DES-78**	620500	4255000	135
DES-36	621500	4254500	138	**DES-79**	620500	4255500	132
DES-37	617000	4257000	128	**DES-80**	619503	4257993	118
DES-38	616450	4256000	143	**DES-81**	618013	4258366	122
DES-39	618030	4256060	130	**DES-82**	617500	4258000	118
DES-40	619015	4255985	130	**DES-83**	618500	4257000	135
DES-41	620530	4254550	143	**DES-84**	619000	4257500	113
DES-42	621500	4253500	150	**DES-85**	619500	4256970	118
DES-43	620500	4256491	127	**DES-86**	618000	4257500	119
DES-87	617500	4257460	129	**DES-133**	619000	4254500	150
DES-88	617500	4256970	125	**DES-134**	619500	4254500	149
DES-89	618000	4256500	126	**DES-135**	619000	4253500	164
DES-90	618000	4255500	130	**DES-136**	619000	4253000	180
DES-91	618519	4256013	124	**DES-137**	619000	4252500	210
DES-92	619000	4255544	132	**DES-138**	619500	4252500	199
DES-93	619500	4256000	124	**DES-139**	619500	4253000	176
DES-94	618967	4256448	119	**DES-140**	619500	4253515	170
DES-95	618048	4254995	142	**DES-141**	618000	4254500	138
DES-96	618500	4255000	136	**DES-142**	617472	4254454	156
DES-97	619000	4255000	136	**DES-143**	617490	4255000	137
DES-98	619500	4255000	142	**DES-144**	617000	4256000	126
DES-99	621500	4255000	120	**DES-145**	617000	4256500	118
DES-100	621000	4255000	132	**DES-146**	617500	4256013	133
DES-101	622000	4254000	138	**DES-147**	617000	4254500	168
DES-102	621500	4254000	139	**DES-148**	617000	4254000	189
DES-103	620000	4254500	143	**DES-149**	617000	4257500	108
DES-104	620000	4255025	139	**DES-150**	617000	4255500	141
DES-105	621000	4254500	139	**DES-151**	616500	4254500	196
DES-106	622000	4254550	138	**DES-152**	616500	4255000	170
DES-107	622530	4254000	137	**DES-153**	616511	4255509	156
DES-108	623000	4254000	135	**DES-154**	616000	4255500	160
DES-109	621000	4253978	142	**DES-155**	616000	4254500	200
DES-110	620500	4254086	155	**DES-156**	616500	4254000	229
DES-111	620000	4253960	162	**DES-157**	617500	4255500	139
DES-112	620000	4253500	170	**DES-158**	616500	4256500	125
DES-113	620000	4252500	189	**DES-159**	616500	4257000	112
DES-114	620500	4252500	189	**DES-160**	616500	4257550	118
DES-115	621000	4252500	168	**DES-161**	616500	4257890	124
DES-116	621000	4253000	155	**DES-162**	616000	4257950	114
DES-117	621000	4253460	155	**DES-163**	616000	4257500	130
DES-118	620500	4253000	170	**DES-164**	616000	4256488	132
DES-119	620500	4253520	162	**DES-165**	616000	4256000	130
DES-120	622000	4253500	145	**DES-166**	615500	4255210	177
DES-121	621500	4252500	175	**DES-167**	615500	4255600	163
DES-122	621500	4253000	150	**DES-172**	615500	4258000	126
DES-123	622000	4253000	160	**DES-173**	615000	4258024	122
DES-124	622550	4252967	158	**DES-174**	615000	4257500	130
DES-125	622000	4252520	170	**DES-175**	615000	4256500	147
DES-126	622500	4252480	156	**DES-176**	615018	4255978	168
DES-127	622223	4251964	180	**DES-177**	614500	4256518	150

DES-128	621700	4252154	195	**DES-178**	614532	4257010	150
DES-129	617060	4255000	150	**DES-179**	614500	4257500	125
DES-130	616000	4254950	185	**DES-180**	614500	4258022	120
DES-131	619000	4254020	157	**DES-181**	614000	4258000	116
DES-132	619450	4254028	150	**DES-182**	613980	4257472	139
DES-183	614000	4257000	150	**DES-197**	612009	4256509	189
DES-184	614000	4256607	136	**DES-198**	611504	4256518	184
DES-185	613500	4256552	176	**DES-199**	611417	4257015	165
DES-186	613500	4258000	125	**DES-200**	611497	4257500	149
DES-187	613035	4257995	132	**DES-201**	611500	4258000	126

DES-188	613000	4257000	150	**DES-202**	610985	4258009	127
DES-189	613017	4256558	133	**DES-203**	611000	4257500	141
DES-190	612475	4256445	190	**DES-204**	611000	4256476	196
DES-191	612500	4257000	157	**DES-206**	610476	4257000	176
DES-192	612500	4257500	137	**DES-207**	610500	4257500	145
DES-193	612500	4258000	130	**DES-208**	610500	4258000	127
DES-194	612003	4258012	128	**DES-210**	610000	4257000	182
DES-195	612000	4257500	141	**DES-211**	610002	4257504	151
DES-196	612000	4257000	165	**DES-212**	621750	4255518	124

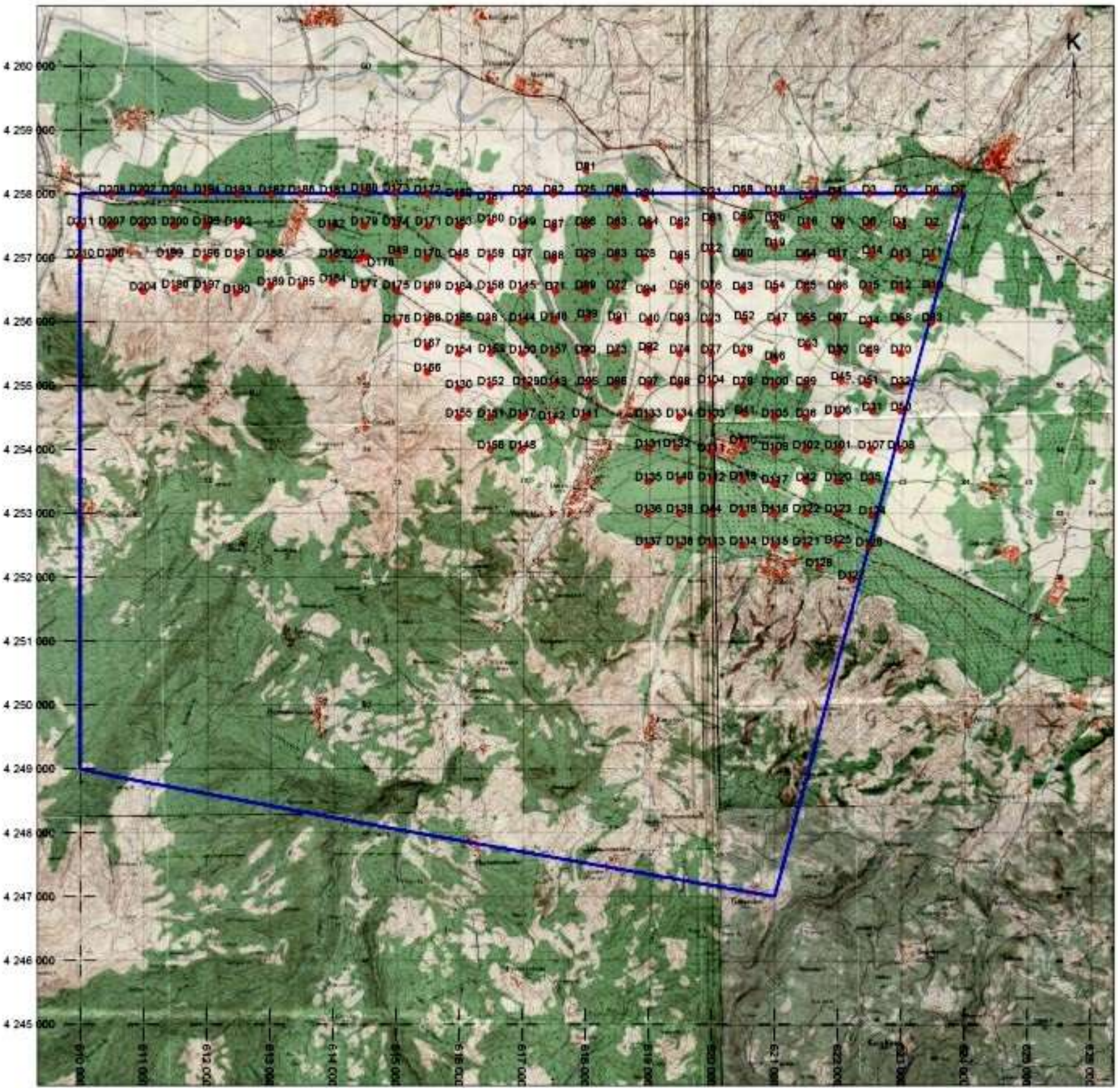

Figure 4. Location map of measurement points of vertical electrical sounding (VES) (UTM -ED50)

2.3 The electrical resistivity maps and interpretation

In this study, along these profiles relationship between, low resistivity inclusions which indicate the presence of thermal activity with tectonic was determined. Resistivity and the former resistivity surveys were re-evaluated on profiles. Apparent isoresistivity map, electrical structural cross-sections, depth maps and topographic basements map were re-created on these profiles and results of these studies were re-evaluated.

The electrical resistivity maps have been re-prepared from all VES locations in the field, in the same depth measurement results, that is they were re-prepared from visible resistivity data. These maps show the different depths resistivity distributions in the field. By the help of the lateral conductive change data, lateral following of the tectonic structure and heat areas in the different depths is possible. To interpret the working area with this thought by analyzing, in accordance with the aim, from the resistivity depth maps prepared for different theory, depths 18 resistivity map were prepared (80 ohm.mis selected max. resistivity value while prepared cross-sections and depth maps for determined min. low resistivity zones).The vertical resistivity distributions of AB/2 = 900 meter, AB/2= 1000 meter, AB/2 = 1100 meter, AB/2= 1200 meter, AB/2 = 1250 meter, AB/2 = 1300 meter, AB/2 = 1400 meter, AB/2= 1500 meter, AB/2 = 1600 meter, AB/2= 1700 meter, AB/2 = 1750 meter, AB/2 = 1800 meter, AB/2 = 1900 meter, AB/2 = 2000, AB/2 = 2100, AB/2 = 2200, AB/2 = 2300, AB/2 = 2400 and 2500 meter theoretical depths in the study area were followed (from Fig.5 to 24).

The geophysical map shows the depth from the surface of the high resistivity layer under the thick and conductive sediment storage, that is, electrical basement (Fig. 25 and 26). The depth data in this map were received from the results of all locations VES curves using EarthImager 1D software re-evaluations. The depths in this map are equal with the basement rocks depth from the surface. The depth data in the map shows the total thickness of the sedimentary rocks on the metamorphic rocks. Bed rock topography and the structure of the basin in the depth size in the depth map can be easily followed. By this reason, the geophysical survey results are the important sources in the determining stage of especially new wells.

2.3.1. Interpretation and resistivity maps of shallow depths

In the Kavaklıdere geothermal field, the depth was described as shallow depths between 900-1500 meters. The interpretation related to these lateral resistivity distribution, this layer which shows the shallow depths in the field, the resistivity maps were prepared from AB/2 = 900 meter to AB/2 = 1500 meter (Fig., from 5 to 12). In the shallow depths, partially this is detected and continues to the deep by broadening. The low resistivity which is not related to the geothermal activity directly was correlated with cap rocks. But, the resistivity gradient which was seen in some parts of the field were interpreted as having a direct relation with the geothermal activity. That is, in the resistivity maps which were prepared for the deep levels of the field, the low resistivity which was seen in the upper parts of the zones directly related with the geothermal activity is thought as a reflection of the heat.

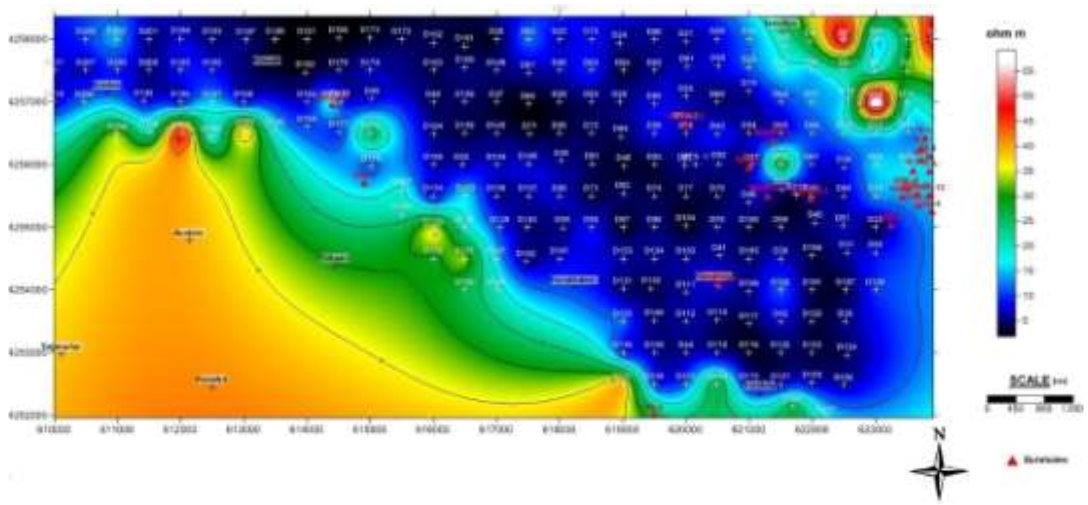

Figure 5. Resistivity depth map of AB/2= 900 meter

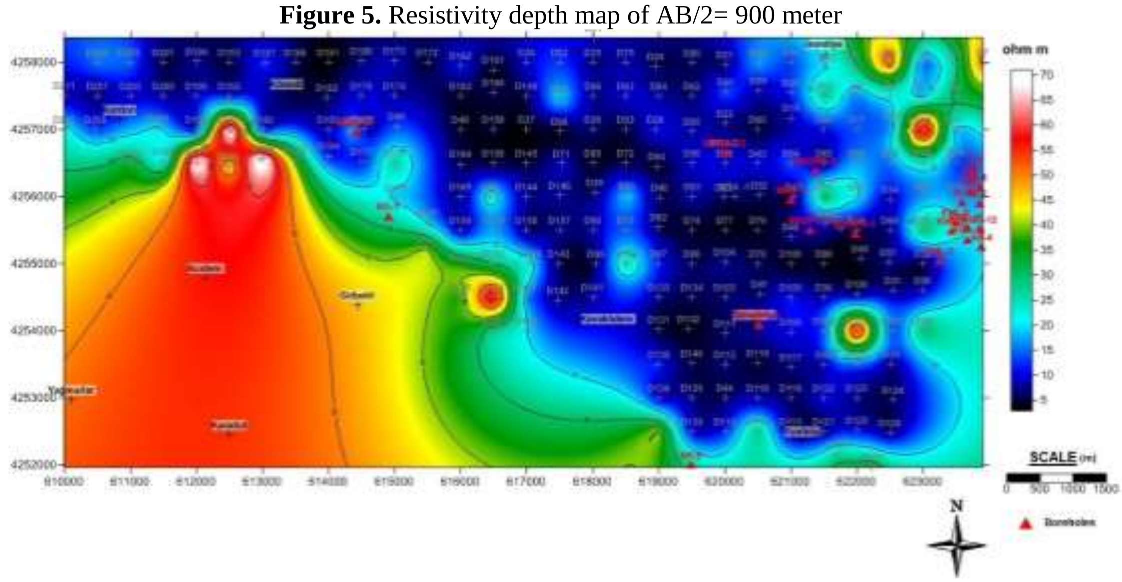

Figure 6. Resistivity depth map of AB/2 = 1000 meter

Paper ID: ART2018930 DOI: 10.21275/ART2018930

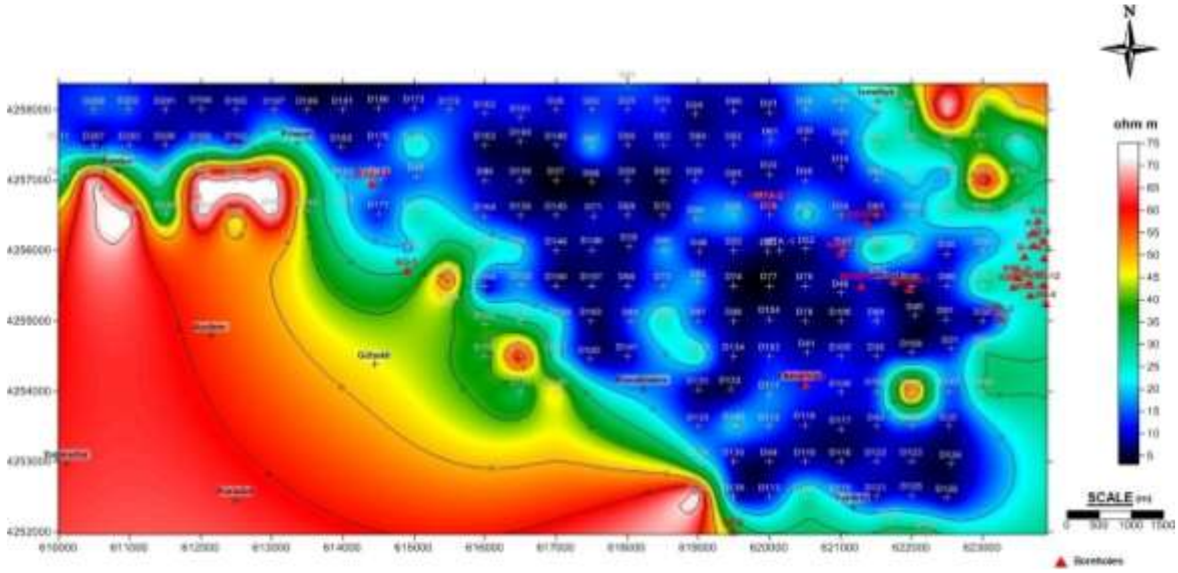

Figure 7. Resistivity depth map of AB/2 = 1100 meter

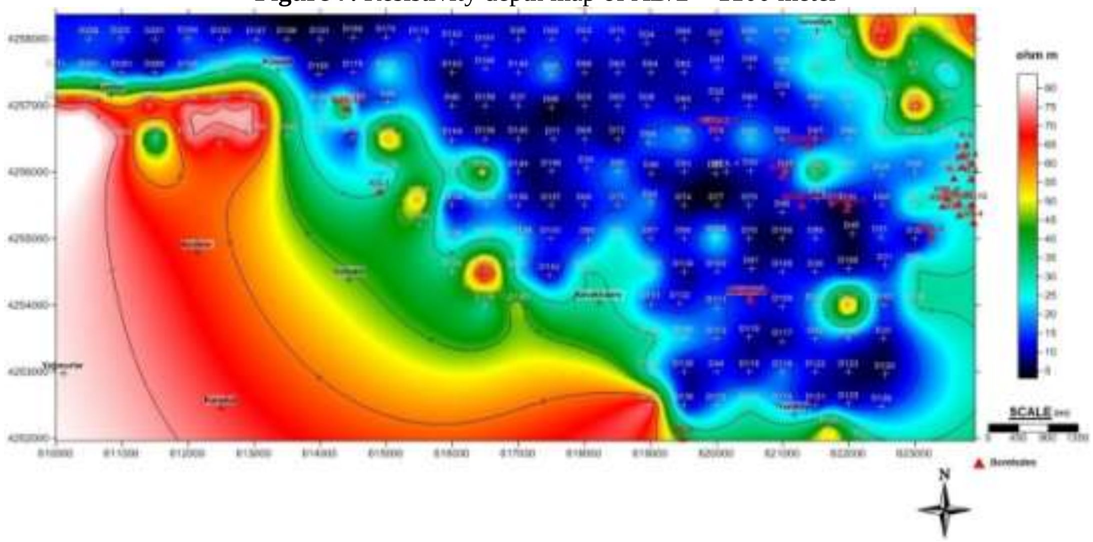

Figure 8. Resistivity depth map of AB/2 = 1200 meter

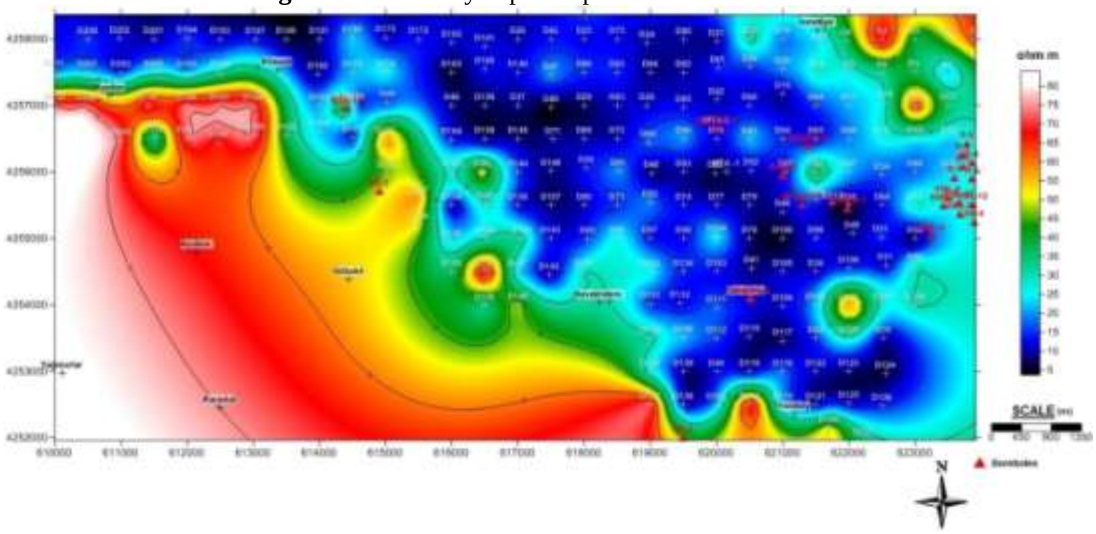

Figure 9. Resistivity depth map of AB/2 = 1250 meter

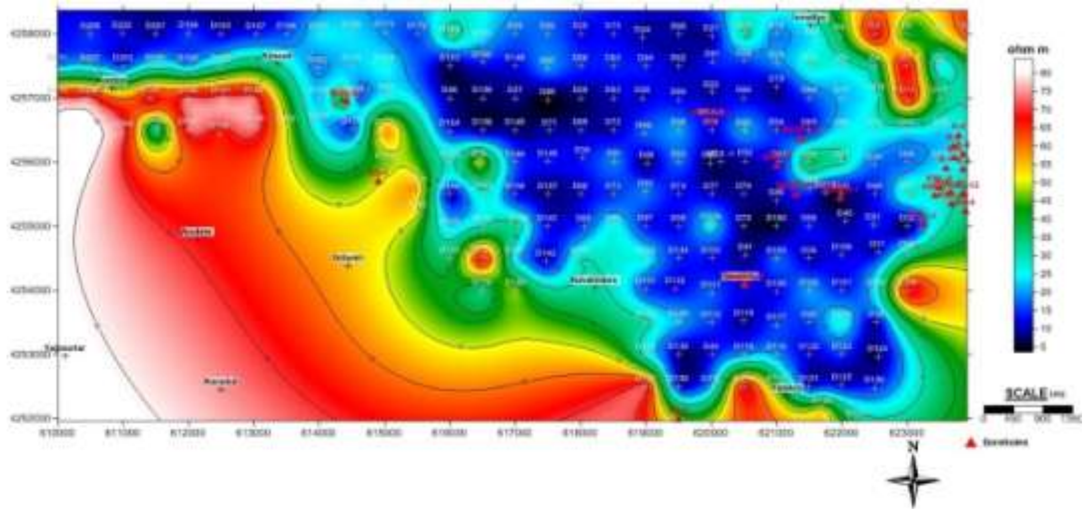

Figure 10. Resistivity depth map of AB/2 = 1300 meter

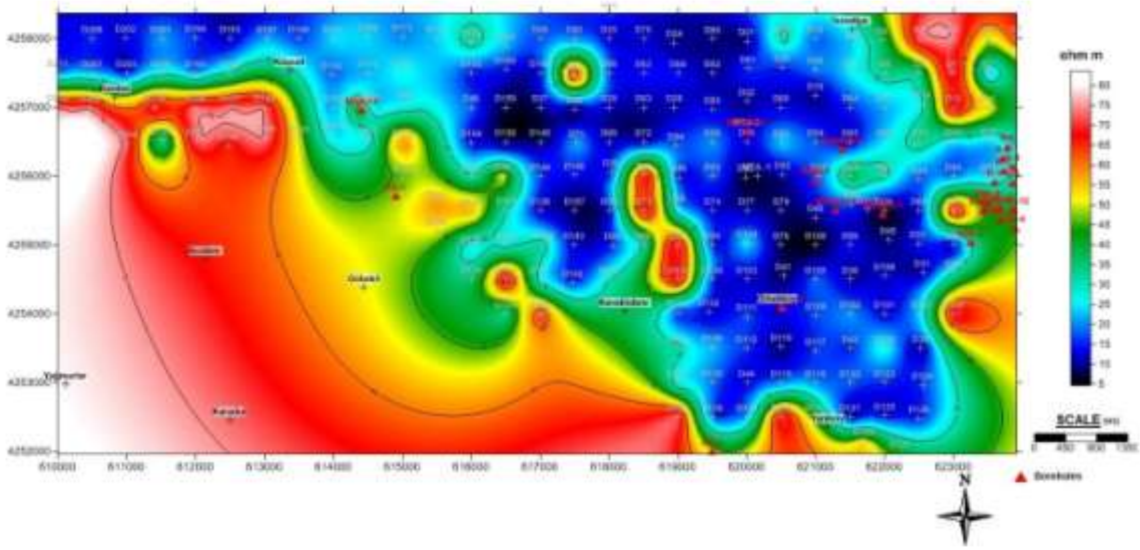

Figure 11. Resistivity depth map of AB/2 = 1400 meter

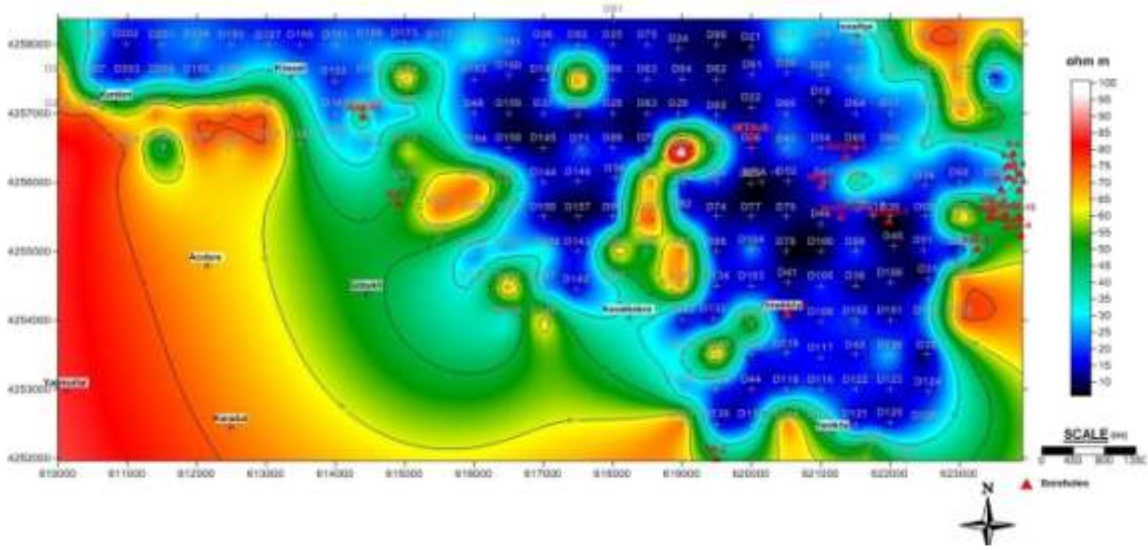

Figure 12. Resistivity depth map of AB/2 = 1500 meter

2.3.2. Interpretations and resistivity maps of deep depths

In the Kavaklıdere geothermal field, the depth described as deep depths between 1500-2500 meters. The interpretation related to these lateral resistivity distribution, this layer which shows the deep depths in the field, the resistivity maps were prepared from AB/2 = 1500 meter to AB/2 = 2500 meter (Fig., from 13 to 23). The low resistivity closure which was determined at the Nort-Northeastern part of the field.

In AB/2= 1500 and 1600 meters theoretical depths, at the Nort-Northeasthern part of the field low resistivity was clear and still has a local appearance. Considering the resistivity distribution which was seen in the resistivity maps representing the 1600 - 1750 meters theoretical depth, the heat effect in these depths was become clear. In the deep depths, the widespreadness of the low resistivity areas related to the fault systems was interpreted in such a way that the depth increases the geothermal potential increases also.

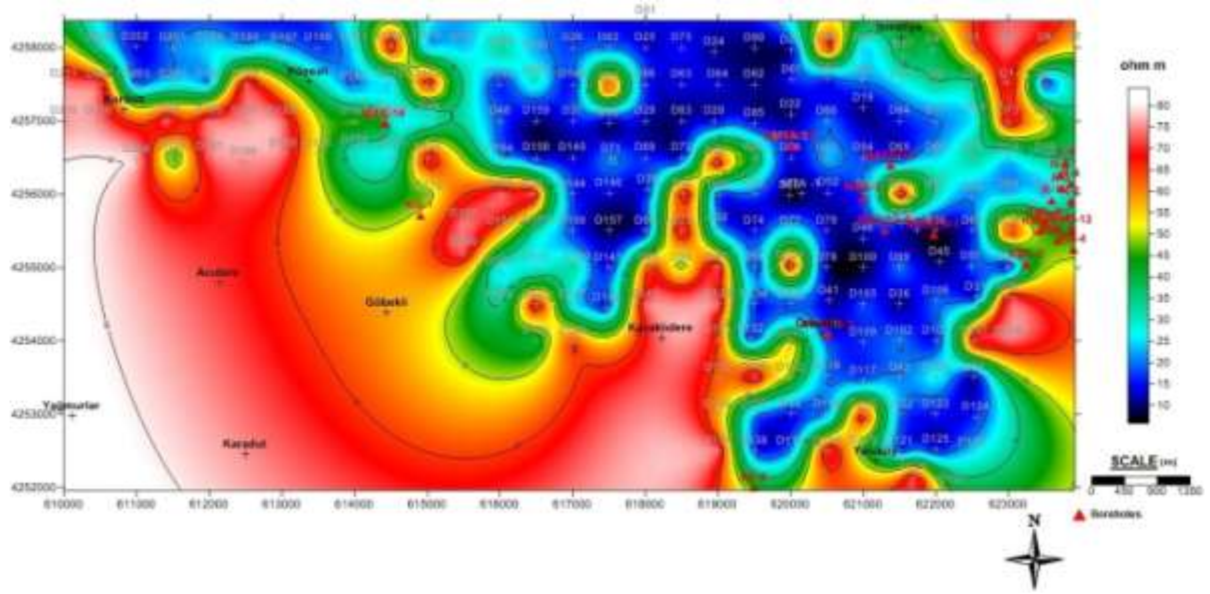

Figure 13. Resistivity depth map of AB/2 = 1600 meter

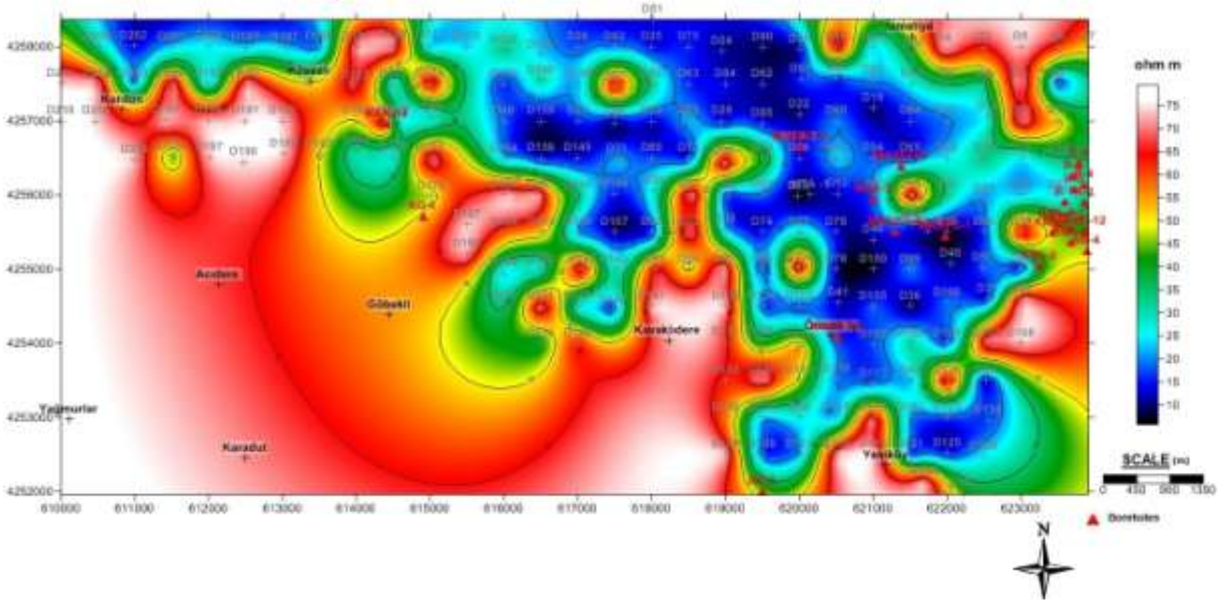

Figure 14: Resistivity depth map of AB/2 = 1700 meter

In the resistivity depth map which represents AB/2= 1750 and AB = 1900 meters theoretical depths, the lowest resistivity distribution was completely determined. In Nort-Northeastern part of the field, the most powerful indicator of the geothermal energy potential was accessed to the lowest values. In the deep depths of the basin filling sediments, measurement of the low resistivity values was described with the electrolytic environment of the high heat liquids in bedrock related to alternation on the cap rocks.

The general appearance in the resistivity depth maps which shows AB/2=1900 and AB/2=2500 meters theoretical depths can be changeable. The related increase of the resistivity values in these maps showed that accessing to the basic units in these levels. But, the resistivity which was seen in these maps was not showed the complete resistivity of the basement units. The falling down of the resistivity to low values, the more sediment thickness in the field, and accordingly increasing the basement depth camouflaged the visible resistivity values.

Paper ID: ART2018930 DOI: 10.21275/ART2018930

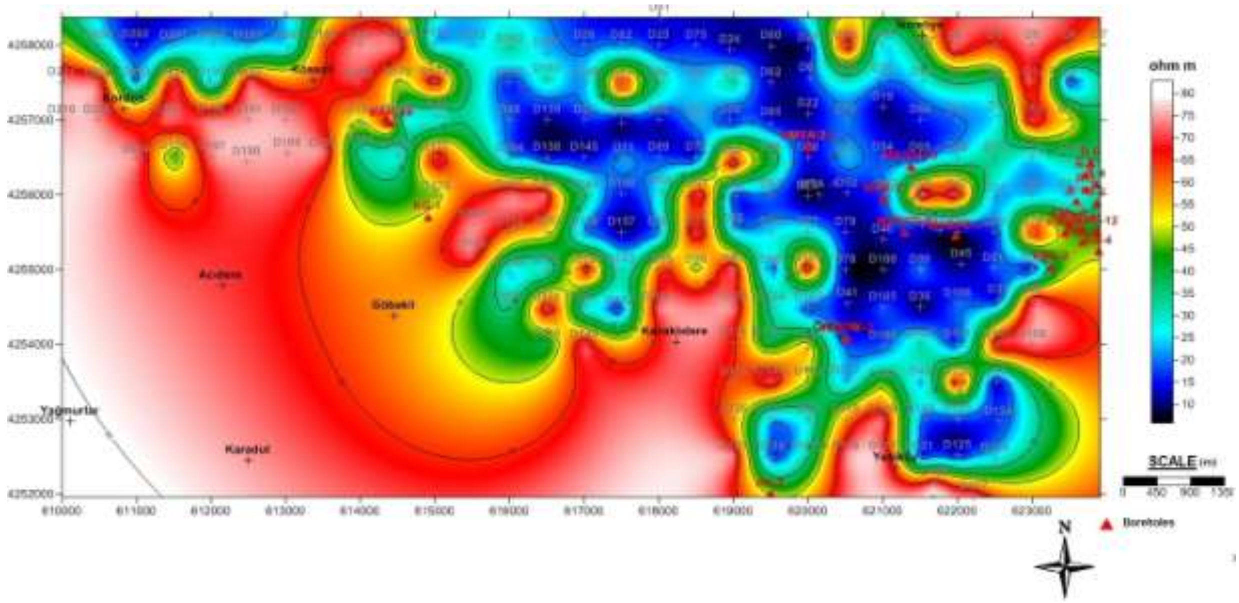

Figure 15. Resistivity depth map of AB/2 = 1750 meter

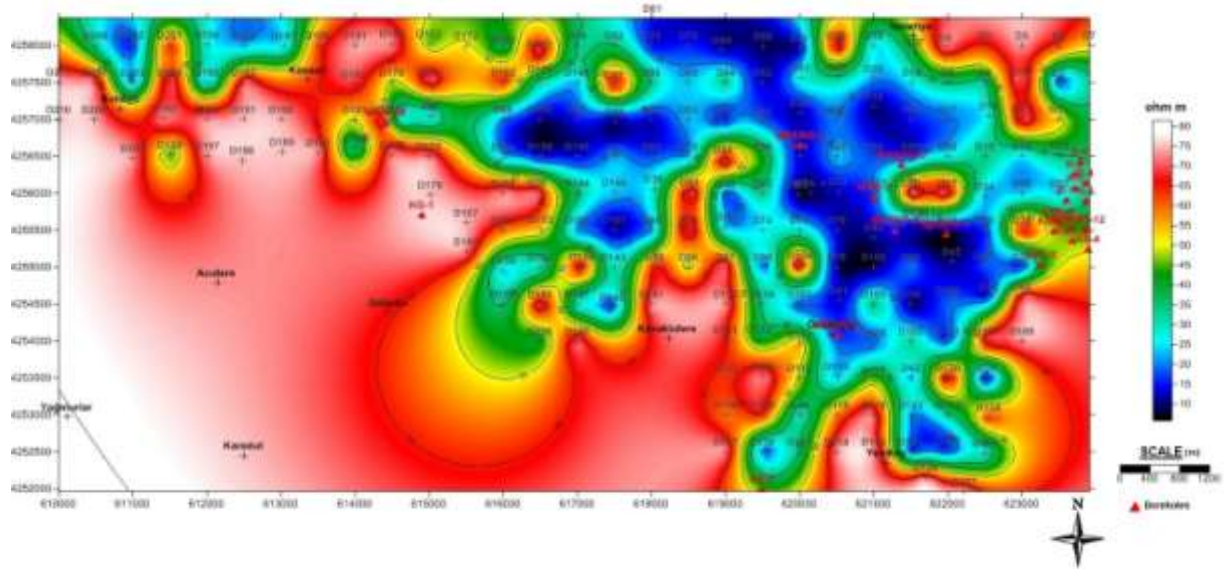

Figure 16. Resistivity depth map of AB/2 = 1800 meter

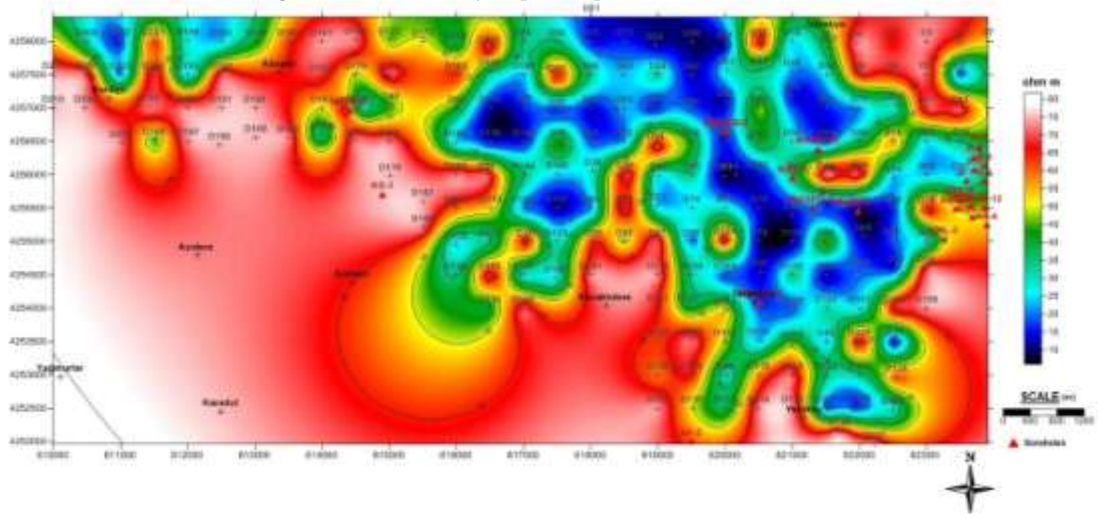

Figure 17. Resistivity depth map of AB/2= 1900 meter

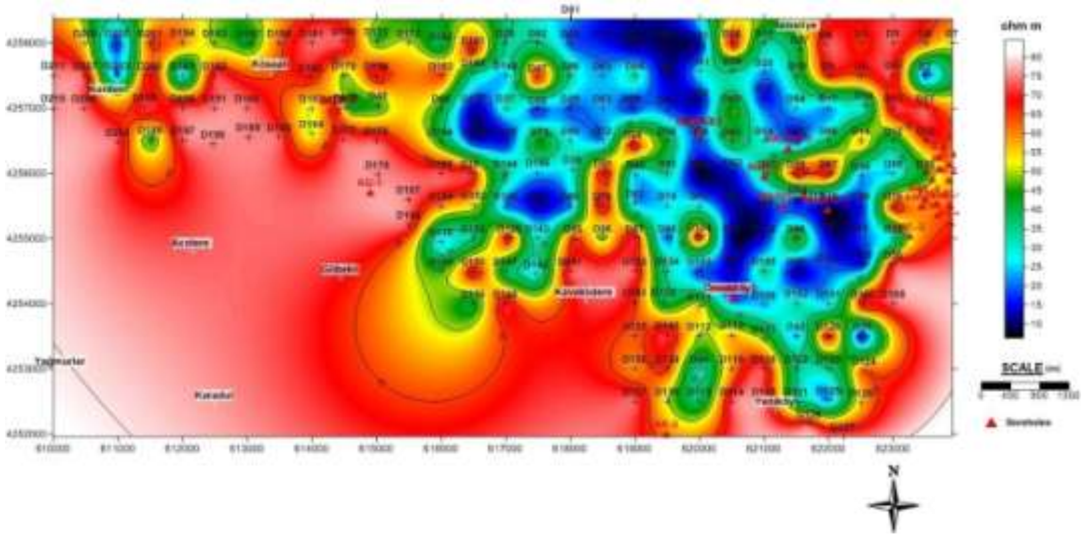

Figure 18. Resistivity depth map of AB/2 = 2000 meter

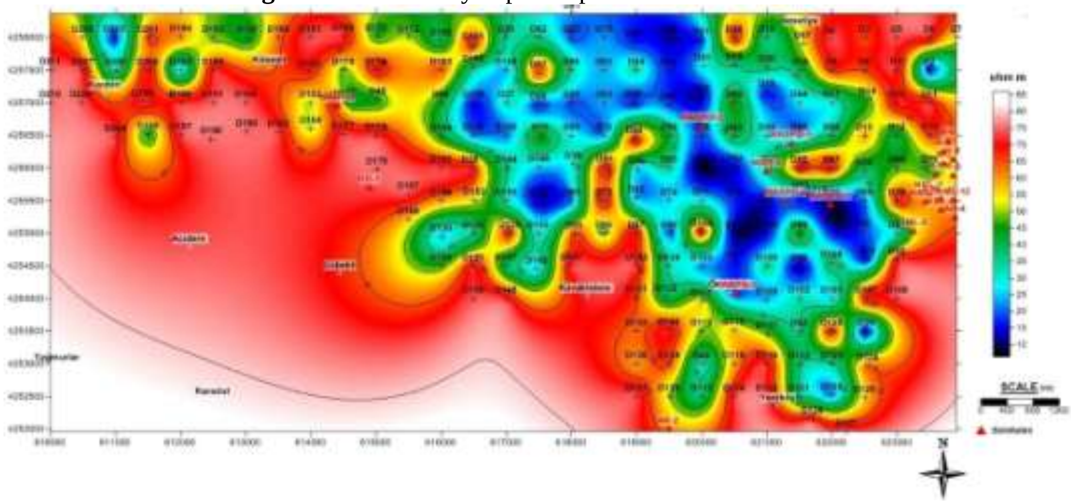

Figure 19. Resistivity depth map of AB/2 = 2100 meter

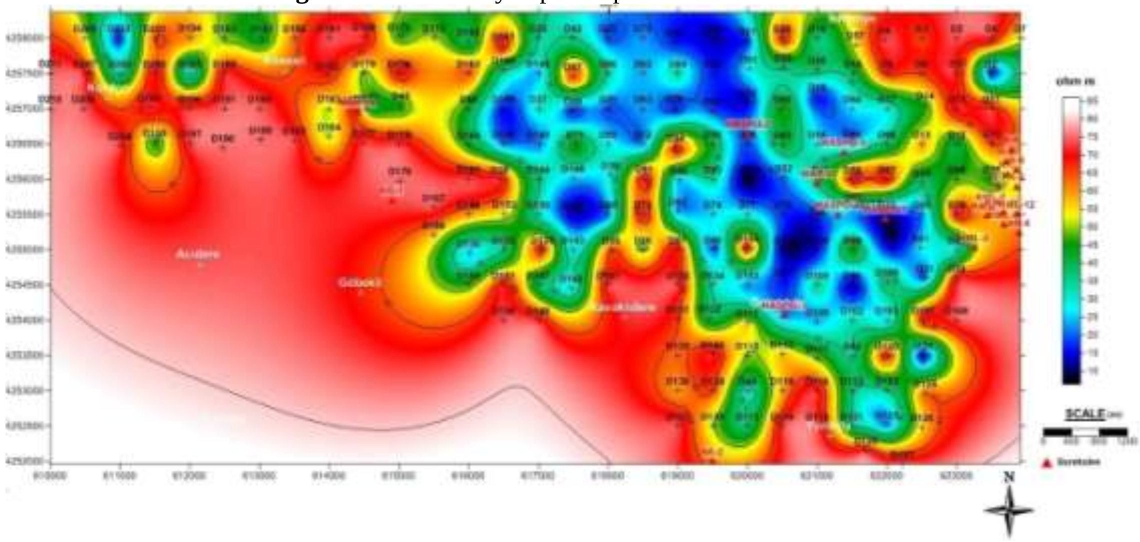

Figure 20. Resistivity depth map of AB/2 = 2200 meter

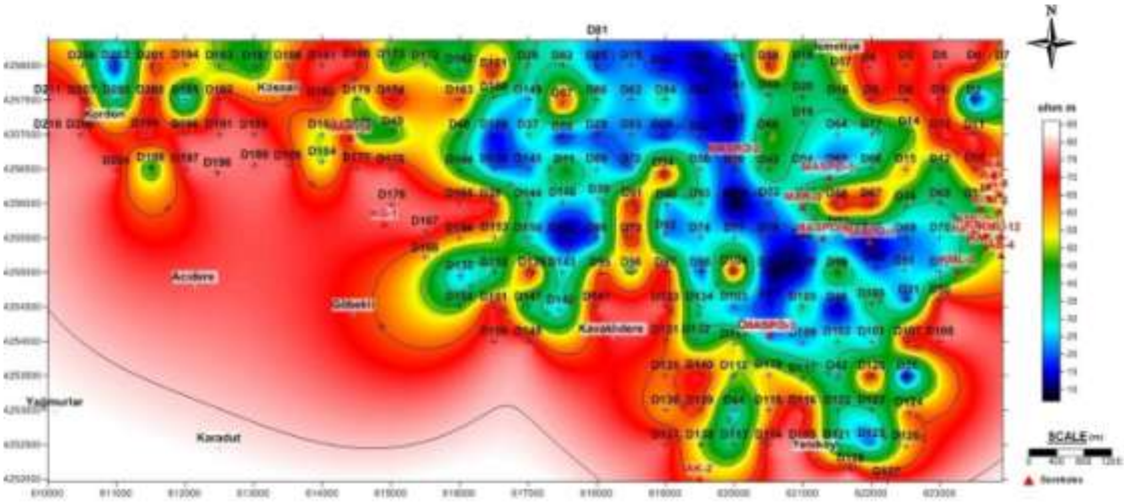

Figure 21. Resistivity depth map of AB/2 = 2300 meter

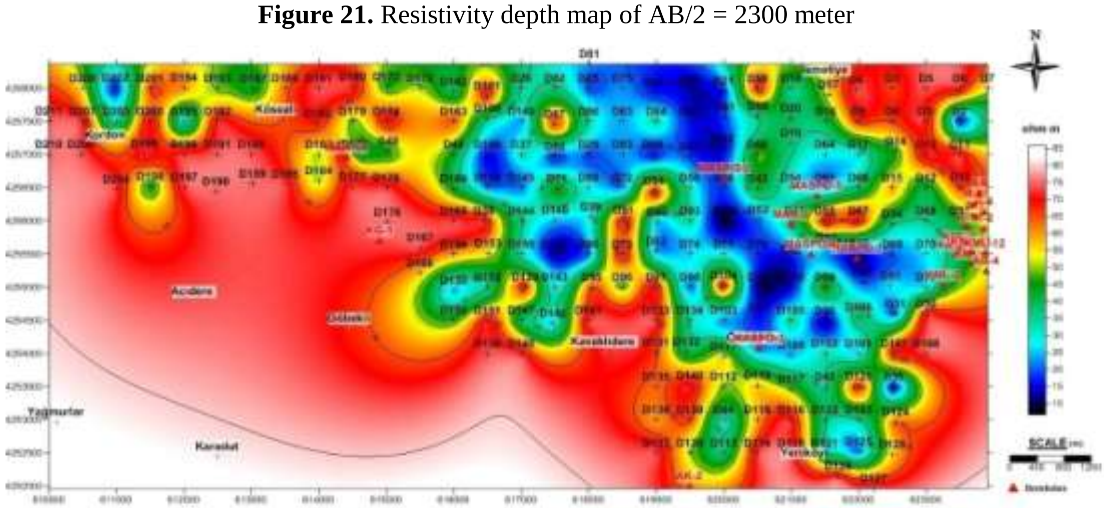

Figure 22. Resistivity depth map of AB/2 = 2400 meter

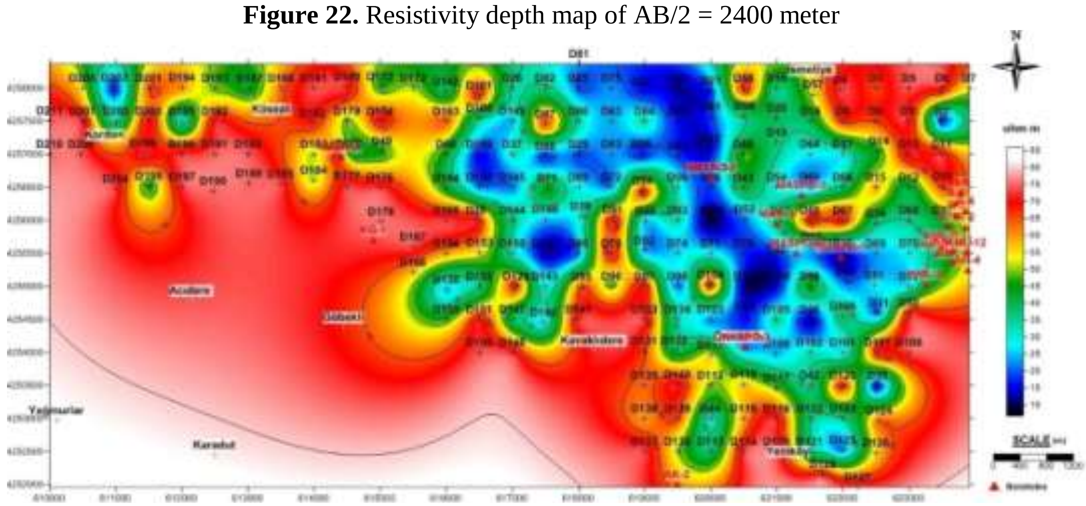

Figure 23. Resistivity depth map of AB/2= 2500 meter

2.3.3. Map and interpretation of basement depth

Geoelectric basement with the high resistivity value was correlated with Menderes metamorphics which originates the study area's basement. At the places where the base was deep if the thickness over levels is thin this may cause insufficiency while distinguishing. For this reason insulator level under basement was evaluated as geoelectric basement. From the found basement depths, basement rock depth or basement topography maps could be prepared. If a basement topography was going to be prepared then from the depth found from each location, that locations elevation would be calculated and by this way that locations elevation could be found. Basement topography map will be derivated from the elevation value found for each location. In the basement depth map, the depths found by 1D model used directly. The distribution of the contour lines in the basement depth map show compability with the faults in the field (Fig., 24 and 25).

International Journal of Science and Research (IJSR)
ISSN (Online): 2319-7064
Index Copernicus Value (2016): 79.57 | Impact Factor (2015): 6.391

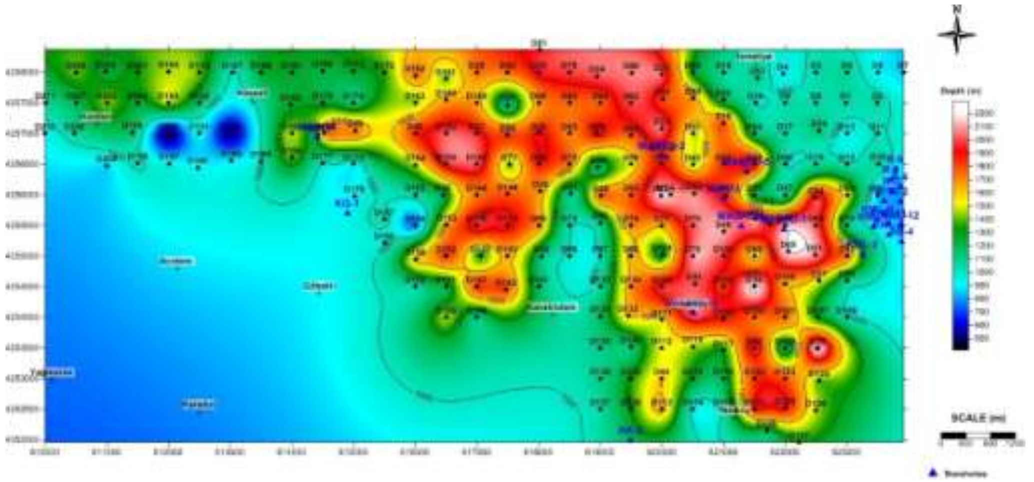

Figure 24. Map of basement depth

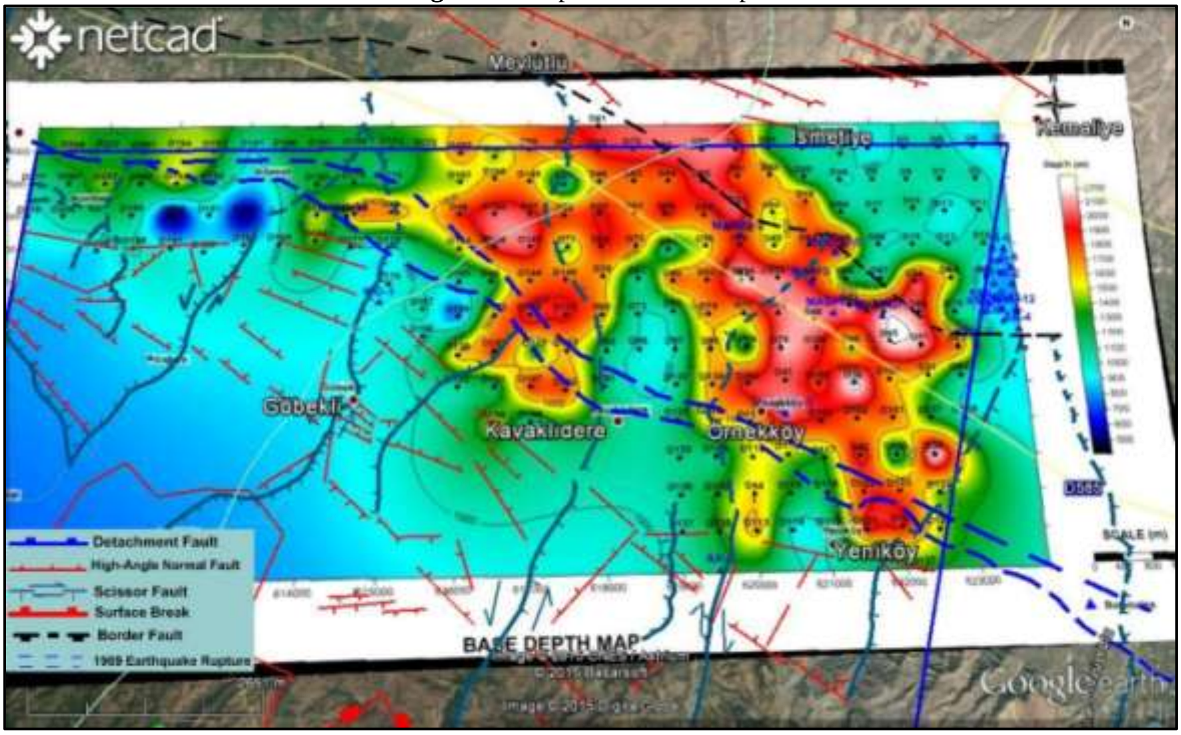

Figure 25. Correlation of basement depth with faults in the study area

2.4. Resistivity cross-sections and interpretation

Resistivity cross-sections were prepared from the resistivity data determined from the results of the measurements of all levels, in all the VES locations throughout the profile. These cross-sections were shown both horizontal and vertical orientations resistivity distributions. It is possible to follow the tectonic structure and heat areas in the theoretical depth size in the part from which the profile passes of the resistivity vertical change. To interpret the Kavaklıdere geothermal field, resistivity cross-sections as compability with tectonic orientations were prepared (Fig., from 26 to 43).

The geoelectrical cross-sections, at the end of the evaluation of VES graphics measured throughout the profile, real resistivities of the layers and beds, thickness and depths were determined. From this data, the geoelectrical cross-sections (model sections) of the profile were prepared. The geoelectrical cross-sections represent the vertical stratigraphic storage and possible tectonic structure throughout the profile with an important approximation. Geoelectrical cross-sections were prepared for a detailed interpretation and evaluation of the area (80 ohm.m is selected max. resistivity value while prepared cross-sections for determined min. low resistivity zones).

Geoelectric cross-sections were prepared in order to reveal possible stratigraphy, fault systems, basement topography and high temperaturely zones along the profile orientations. For this reason, Northwestern-Southeastern and Southwestern profiles were prepared and interpreted.

Numerous horst-graben systems were observed in study area. According to this many fault was originated in study area. Faults are mostly developed in Northwestern-Southeastern and Southwestern-Norteasternorientation. Developed fault systems mostly as each other's follow-up and also they could be evaluated as some faults were branched into several branches.

To interpret the Kavaklıdere geothermal field in NW-SE orientetion 5 cross-sections and SW-NE orientation 9 cross-sections was prepared. In the cross sections, many fault systems were modelled in corresponding zone. Low resistivity zones was developed together with fault systems. In other words higher temprature fluids within faults causes alterations in cap rocks.

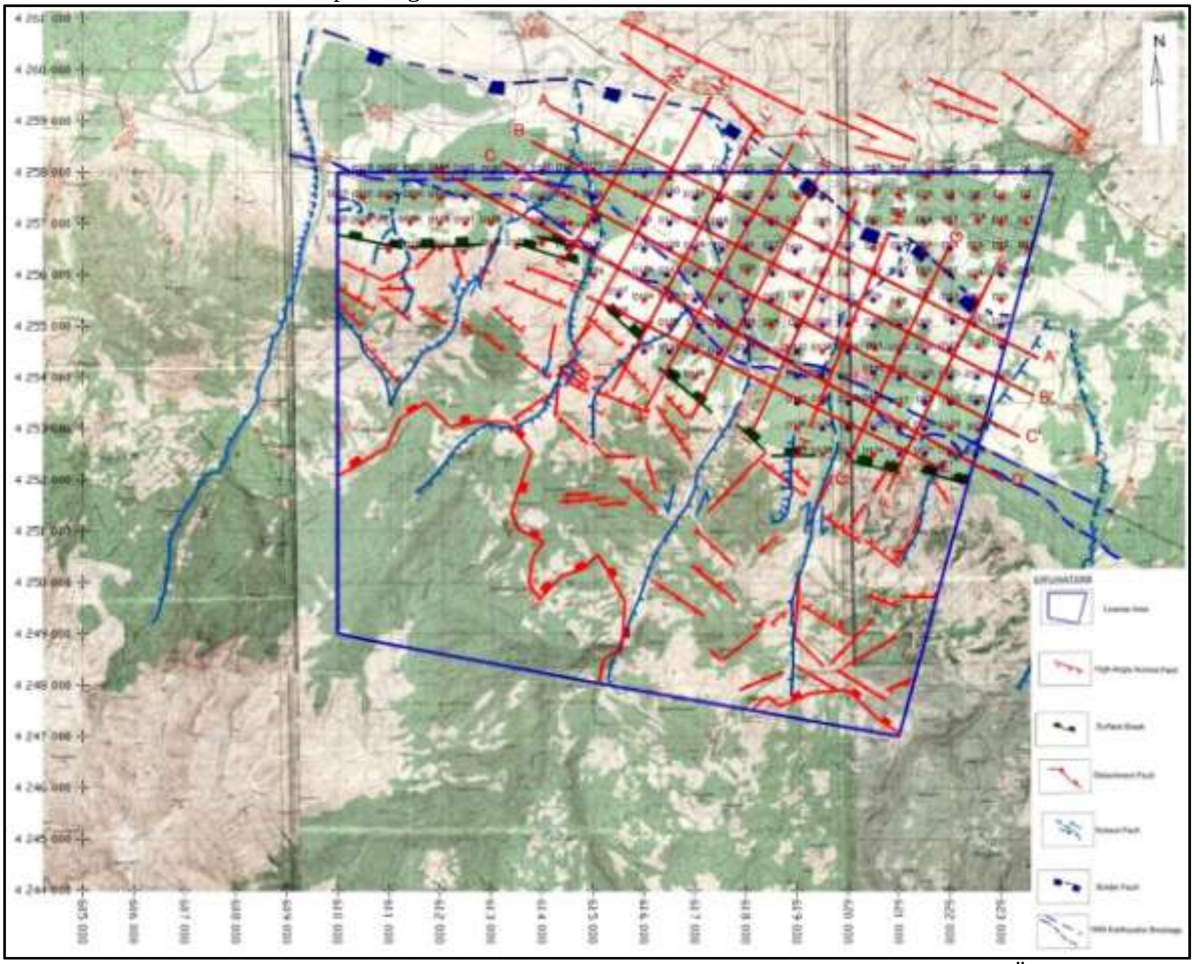

Figure 26. Location map of re-prepared geophysical and geological cross-sections (modified from Özdemir et al., 2016)

International Journal of Science and Research (IJSR)
ISSN (Online): 2319-7064
Index Copernicus Value (2016): 79.57 | Impact Factor (2015): 6.391

Figure 27. Google earth image of re-prepared geophysical and geological cross-sections

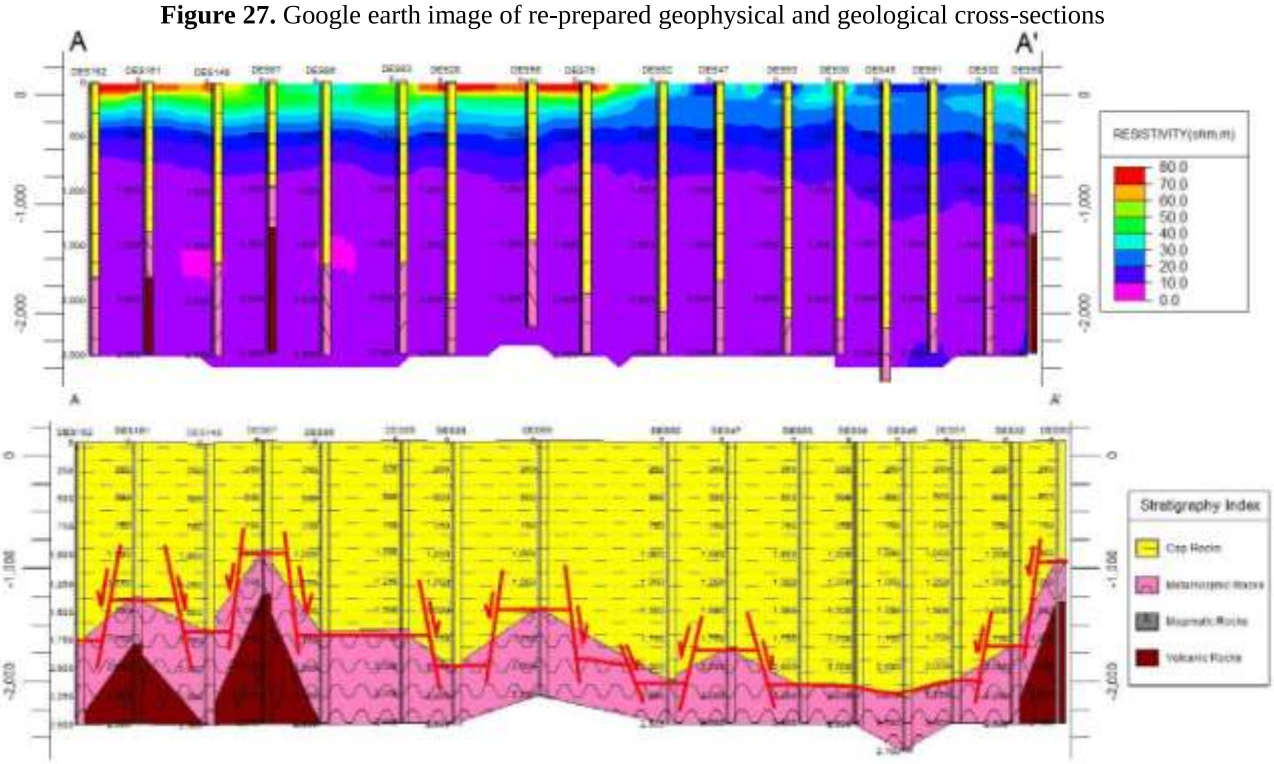

Figure 28. A-A' cross-section and interpretation

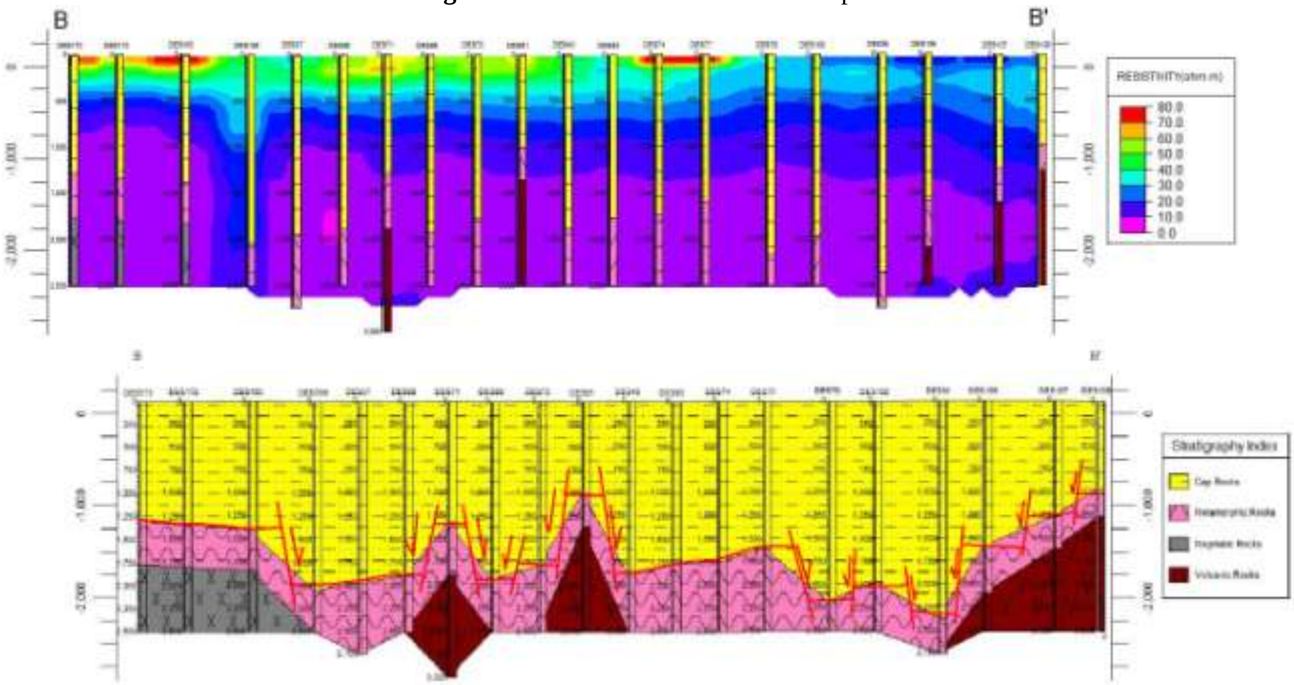

Figure 29. B-B' cross-section and interpretation

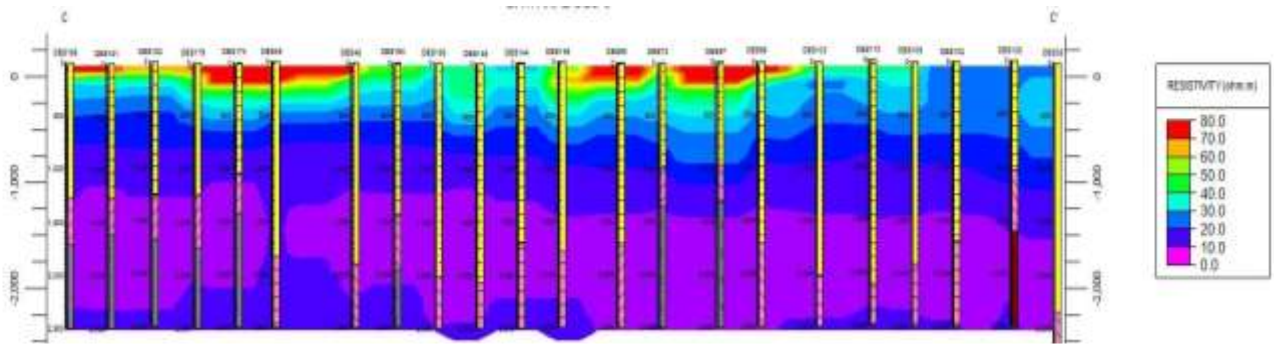

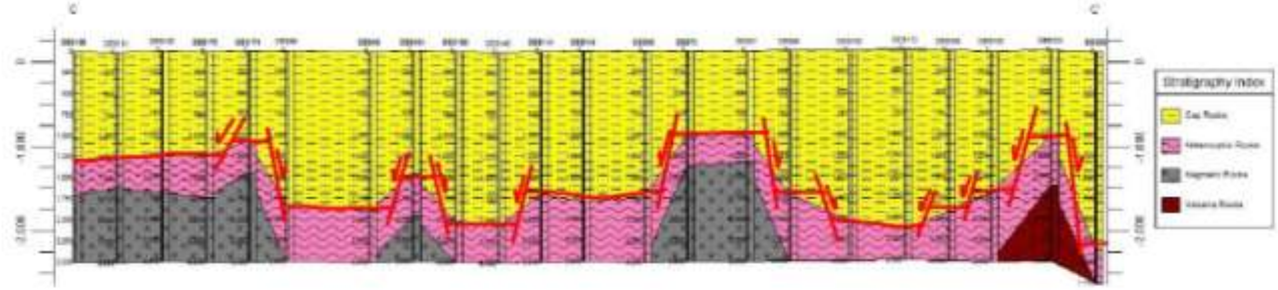

Figure 30. C-C' cross-section and interpretation

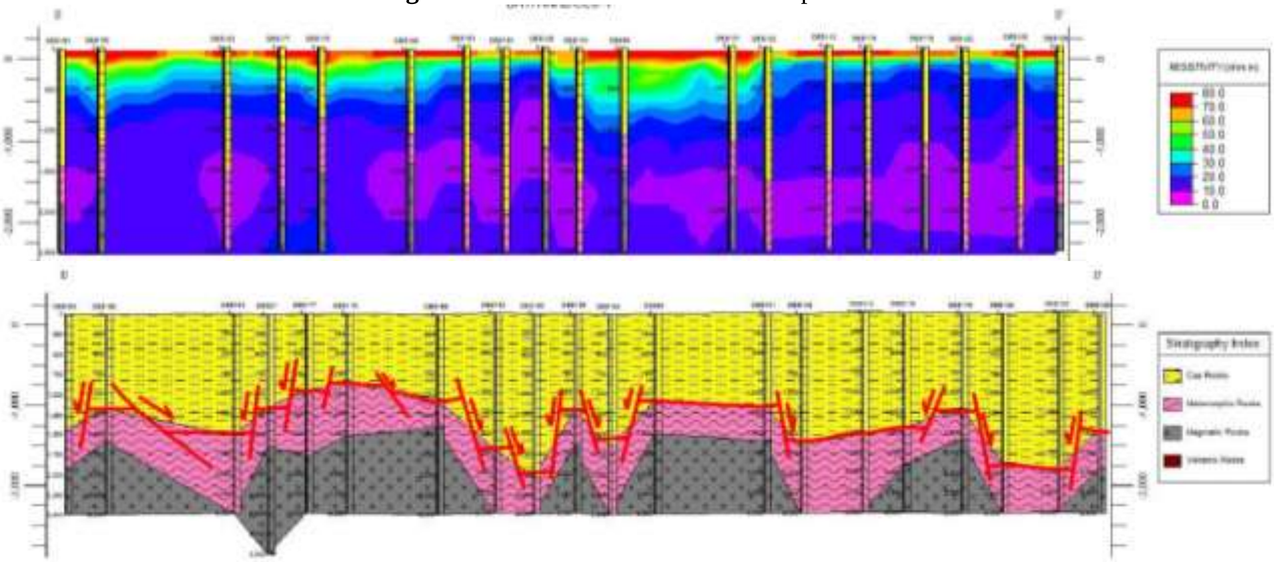

Figure 31. D-D' cross-section and interpretation

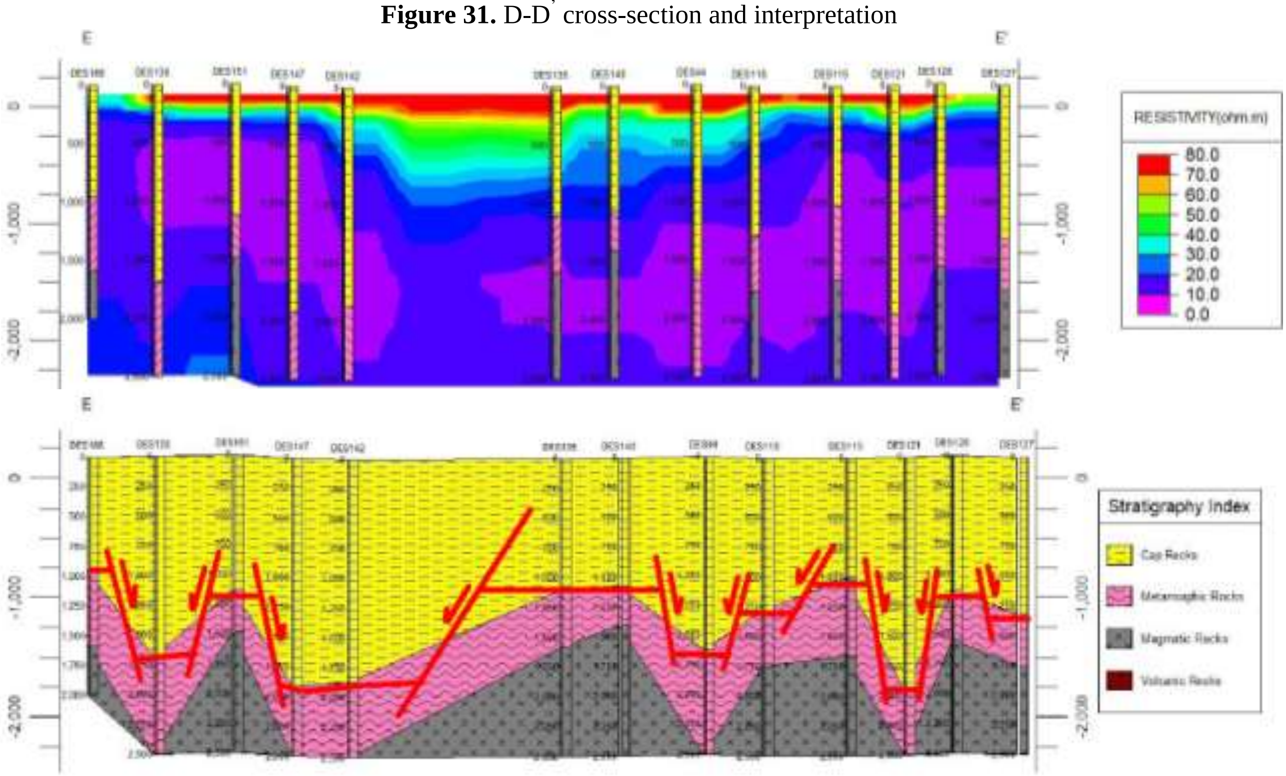

Figure 32. E-E' cross-section and interpretation

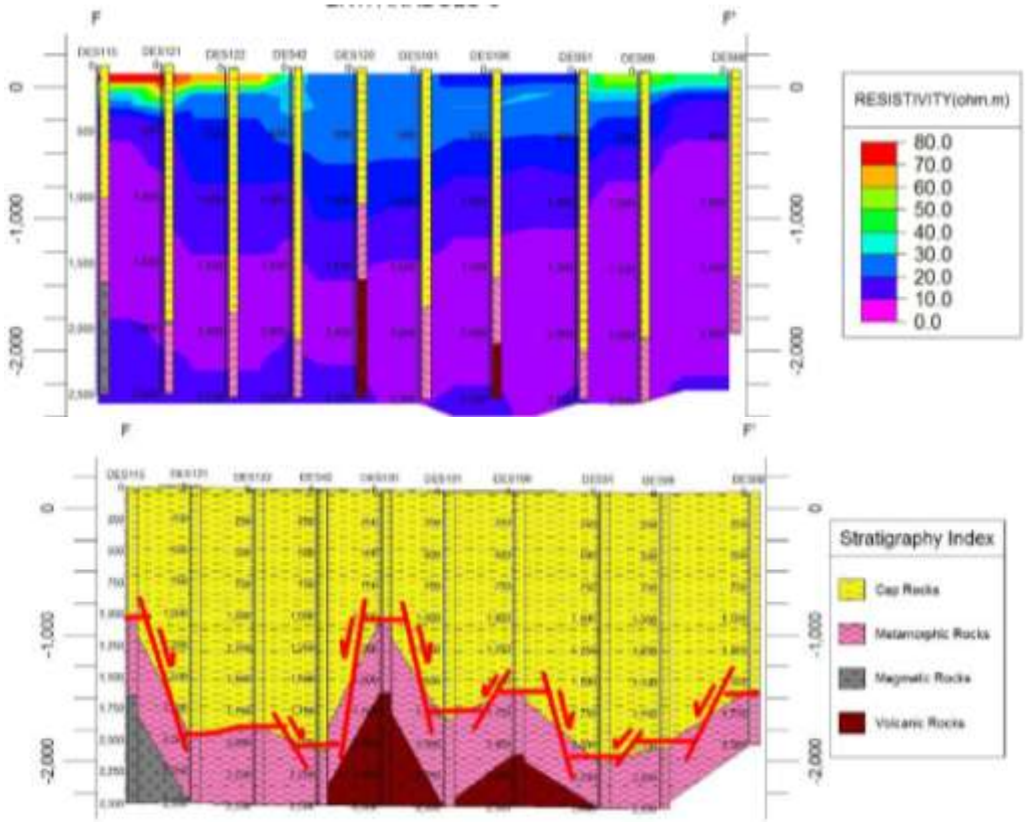

Figure 33. F-F' cross-section and interpretation

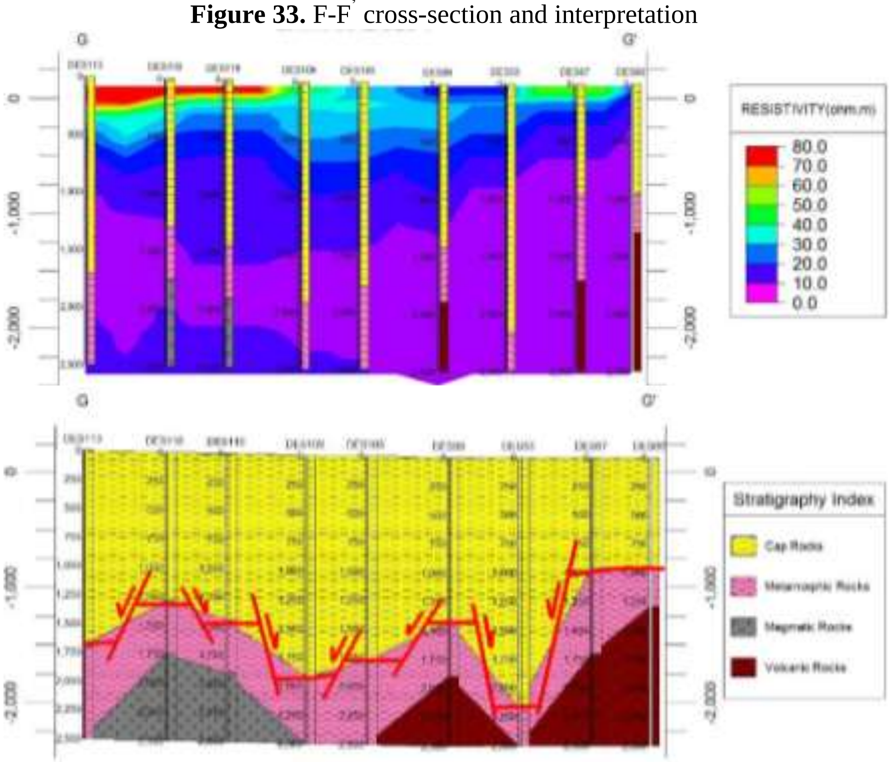

Figure 34. G-G' cross-section and interpretation

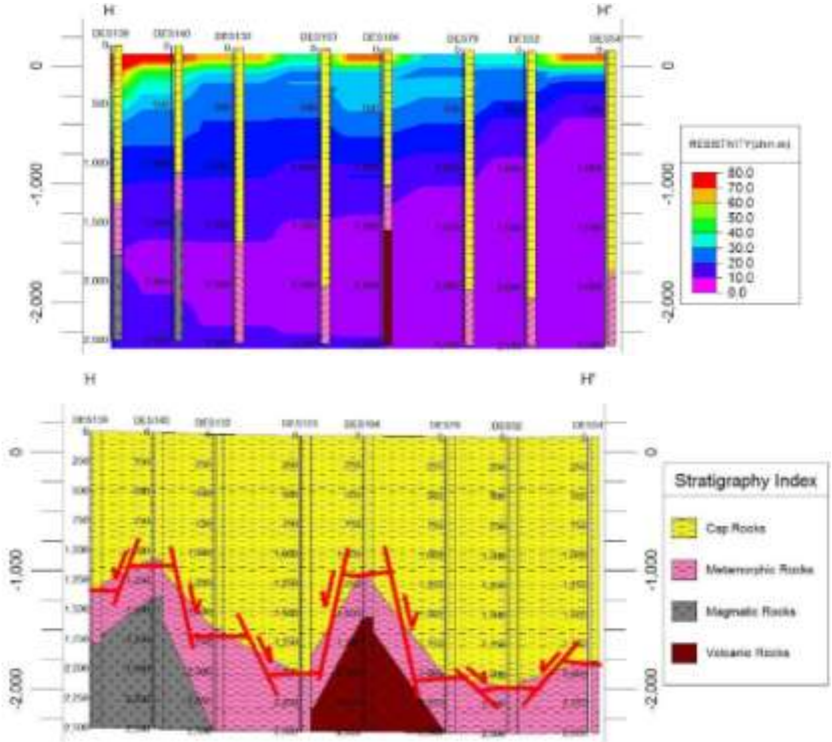

Figure 35. H-H' cross-section and interpretation

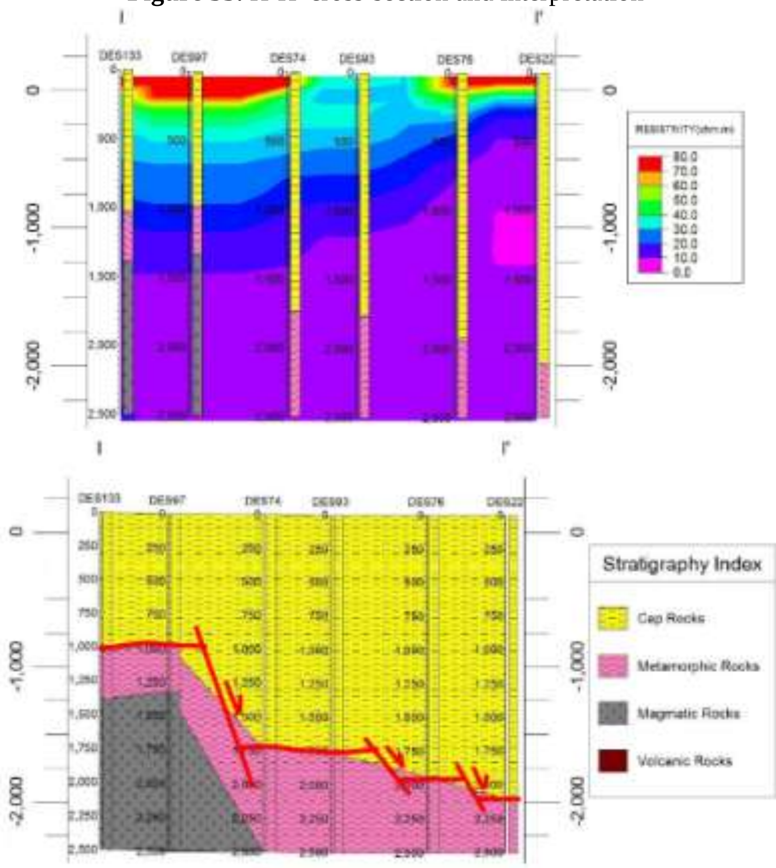

Figure 36. I-I' cross-section and interpretation

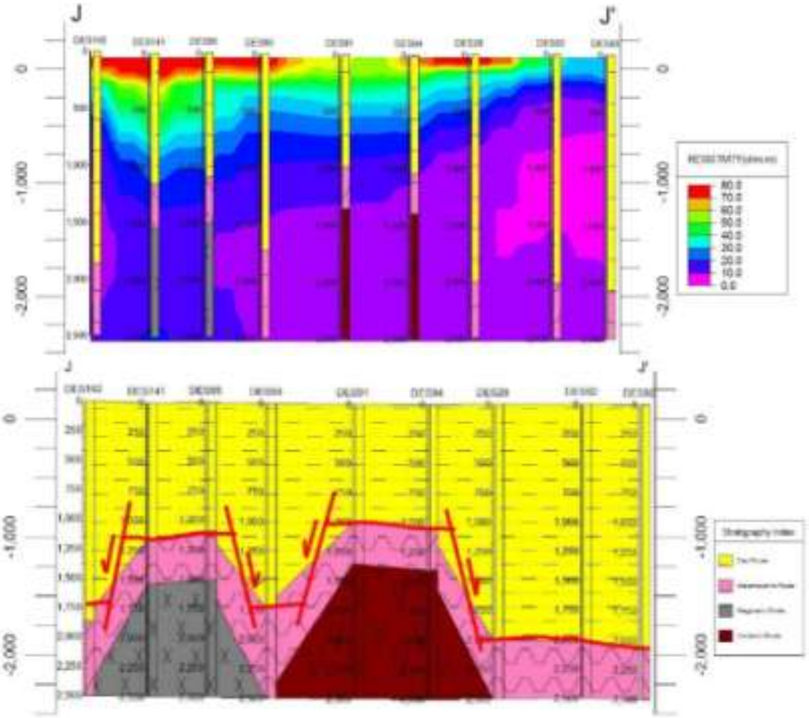

Figure 37. J-J' cross-section and interpretation

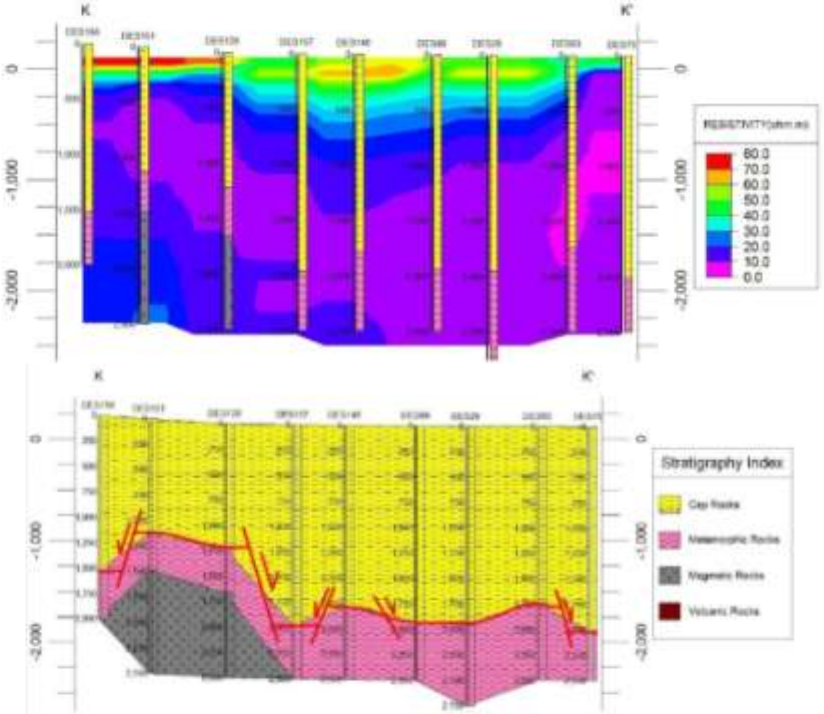

Figure 38. K-K' cross-section and interpretation

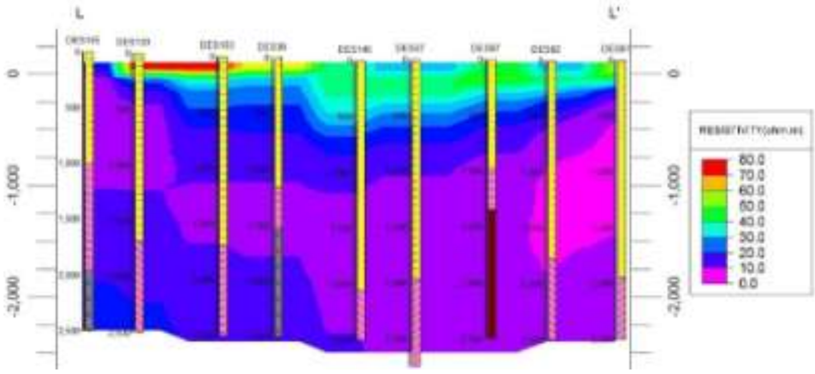

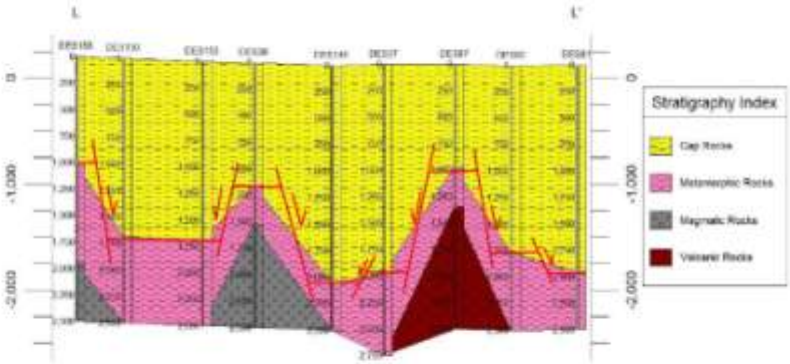

Figure 39. L-L' cross-section and interpretation

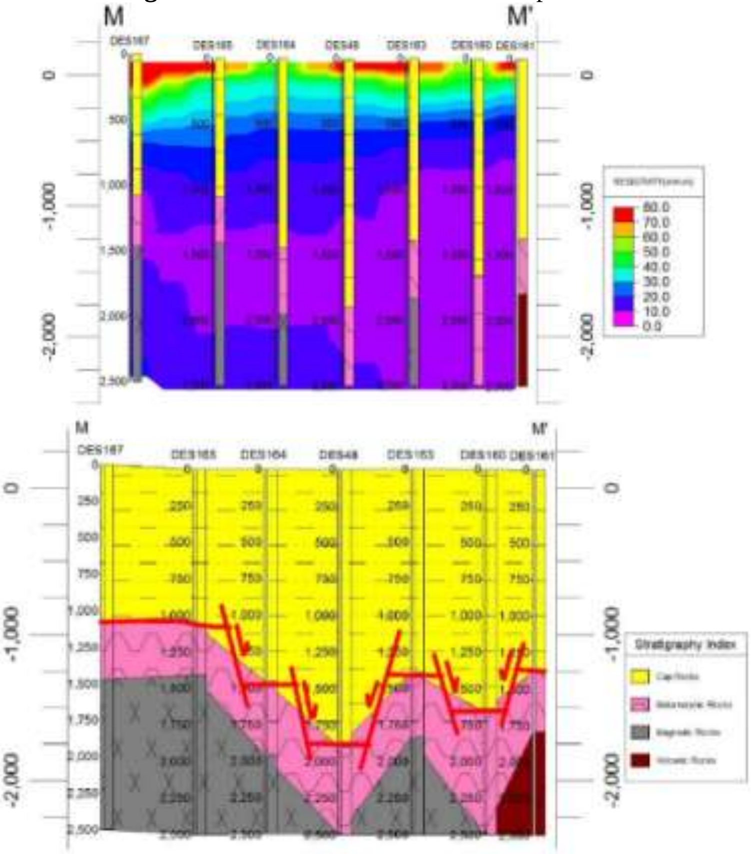

Figure 40: M-M' cross-section and interpretation

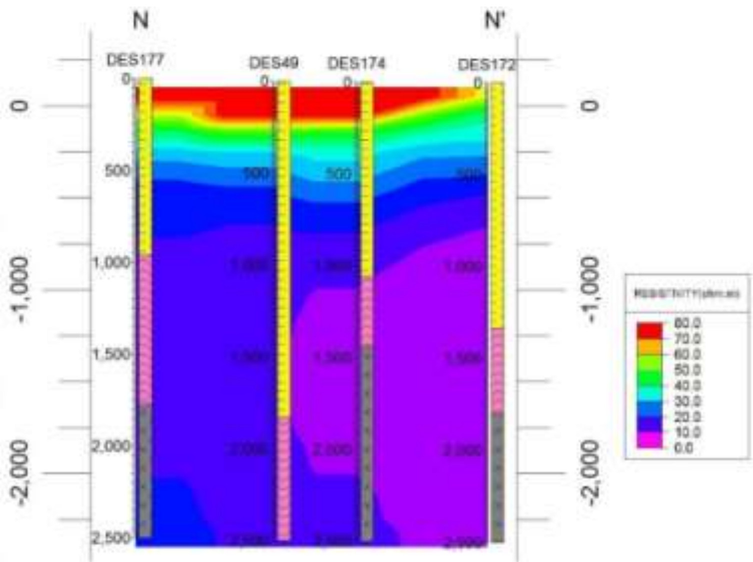

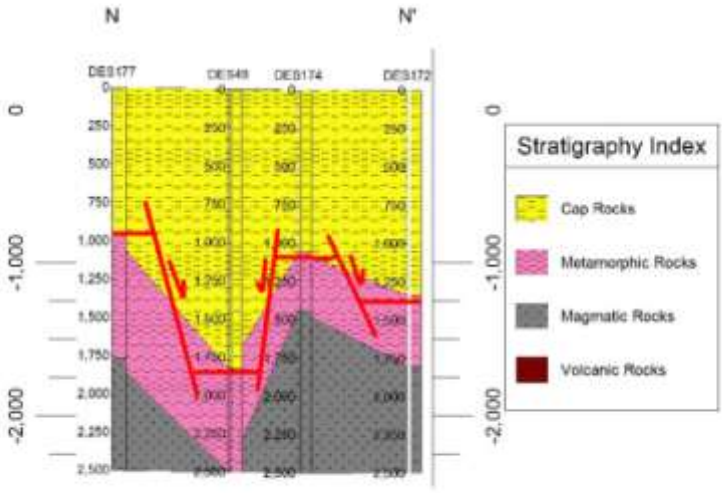

Figure 41: N-N' cross-section and interpretation

To interpret the Kavaklıdere geothermal field, 3D resistivity and stratigraphy models (solid model and fence diagram) as compability with tectonic orientations were prepared (Fig., 42 and 43).

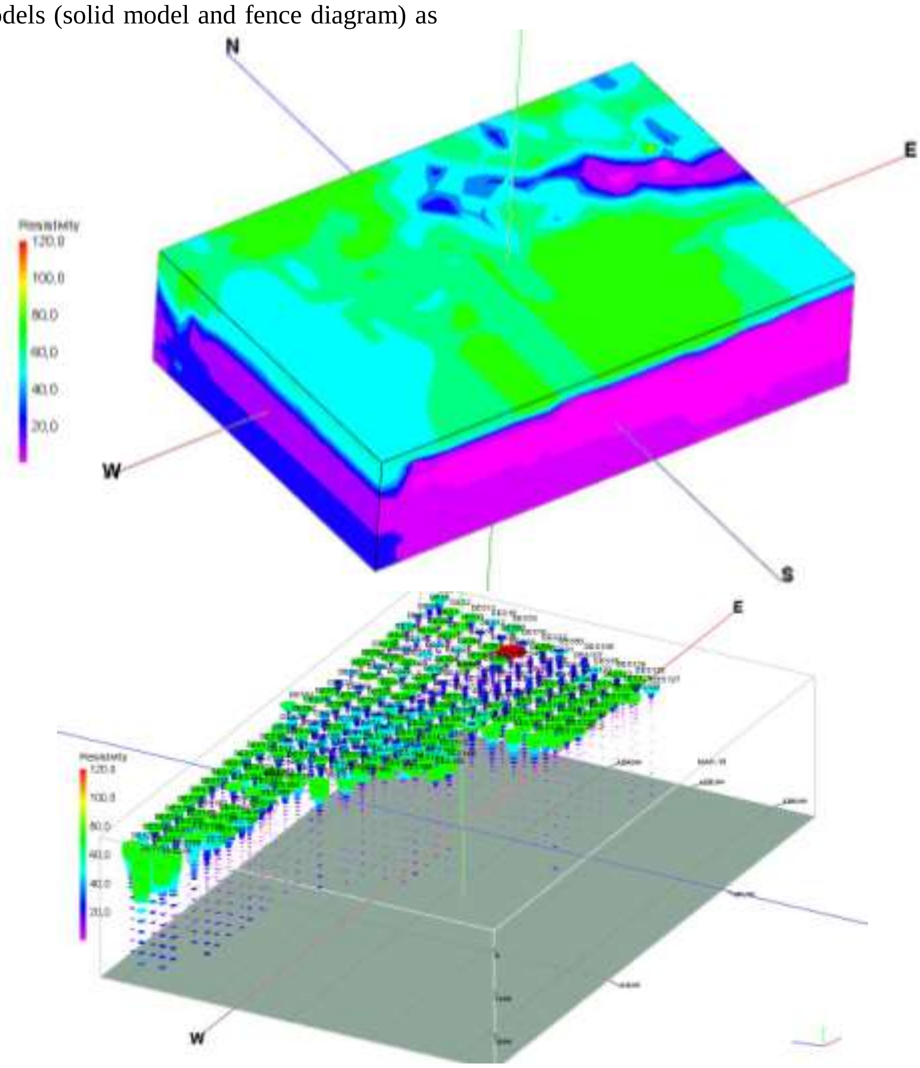

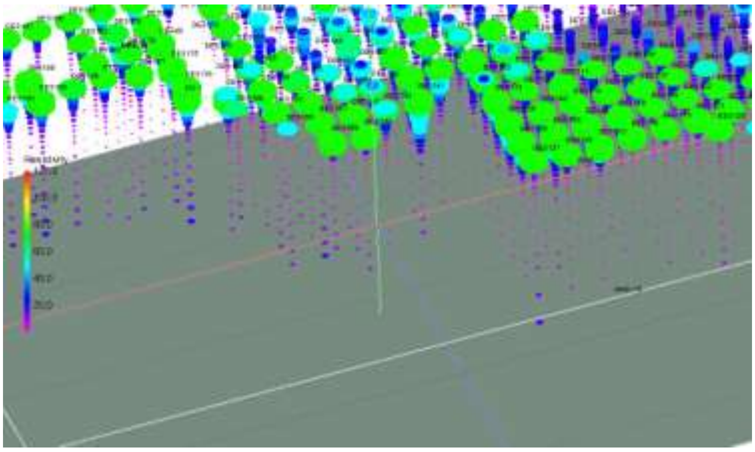

Figure 42: 3D resistivity model of the Kavaklıdere geothermal field

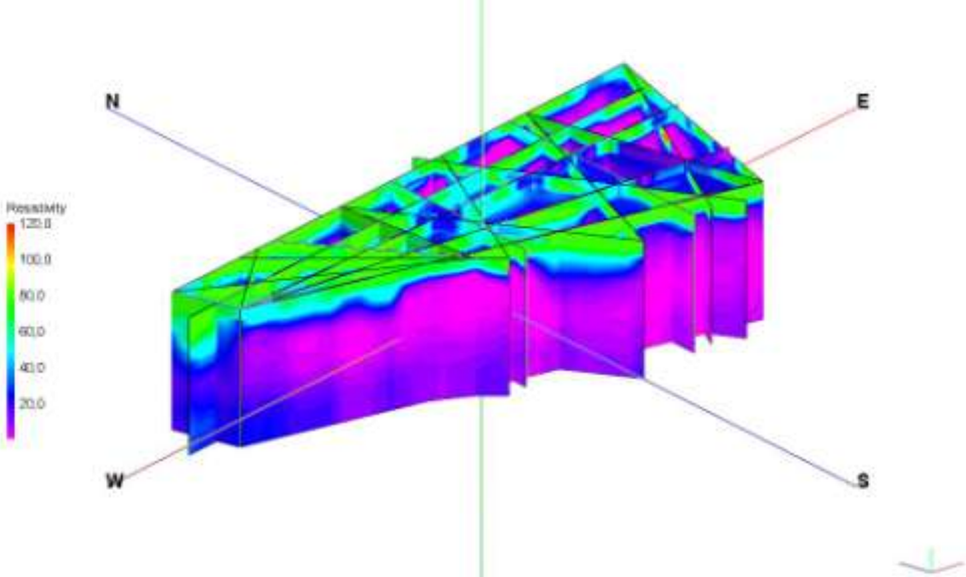

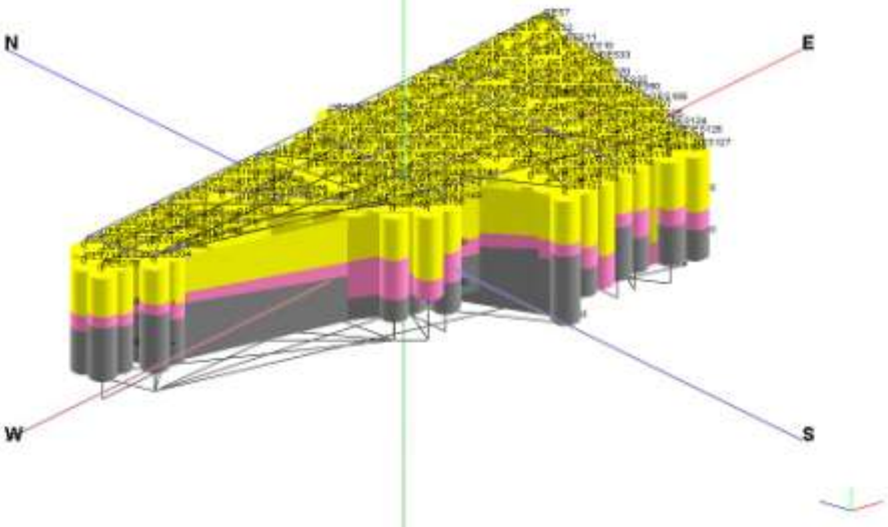

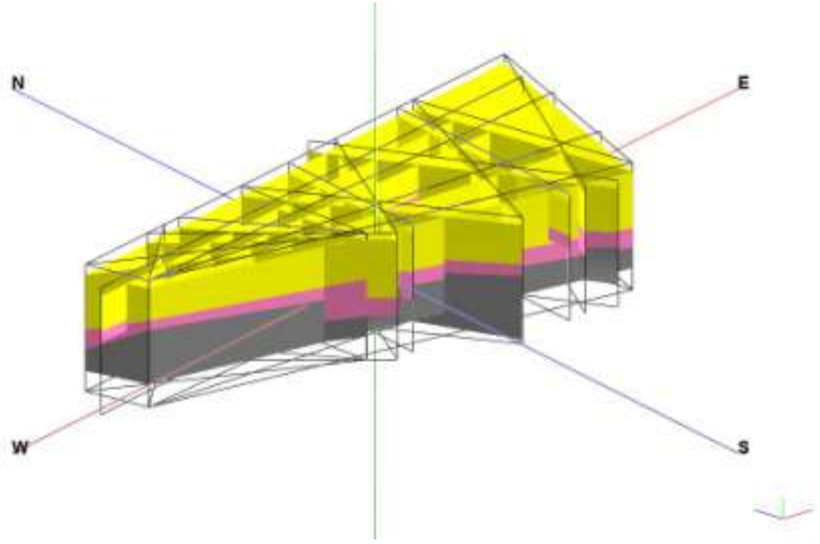

Figure 43: Fence diagram of resistivity and stratigraphy of the Kavaklıdere geothermal field

2.5. Potential Geothermal Reservoirs

Potential geothermal reservoirs were detected at the result of the geophysical measurements made for determining the expected thermal activities at intersection points of the different orientioned faults mostly located at middle and north sides of the study area (Fig. 44; Block 3 and 4). By considering geologic and tectonic compability it was expected to gather fluid with higher temperature and flow from the drillings going to be open.

The geothermal activities at the Kavaklıdere geothermal field appear to lie at the intersections of minor northerly striking sinistral normal transfer faults and the Gediz detachment fault. Left steps in the transfer faults at the intersection with the detachment were inferred to represent dilational jogs (i.e., small pull aparts) that provide channelways for geothermal fluids (Fig. 44). The left steps may result from refraction across the detachment surface that results from the mechanical contrast between hanging-wall sedimentary rocks and basement gneisses, marbles, and schists in the footwall. Brecciated marble at these intersections provide good reservoirs for the geothermal fluids. It was determined that the reservoirs as plunging gently northward along the intersection of the detachment fault with the transfer faults. Although this model can account for the shallow reservoir and surface springs, it may not predict the location of the main upwelling that feeds these geothermal systems. Major steps in the Alaşehir frontal fault or complex fault intersections between the transverse faults and WNW-striking normal faults may accommodate upwelling in the Kavaklıdere geothermal field.

High resistivity zones were interpreted to be regions of cooled intrusions with minimum porosity and permeability. This interpretation of cooled intrusions may not be conclusive as the MT data do not cover as a wide area as the gravity data covered with basalts or andesites domes may have high resistivity. Unfractured rocks were marked by intermediate to high density zones and high resistivities. The locations of the reservoir region and dikes and sillsthat provide heating for the system were interpreted. These models present an improved and more complete picture of the upper crustal structure of the Kavaklıdere geothermal fields by identifying all the features related to the geothermal system. Geological and geophysical structure of the Kavaklıdere geothermal field is very simalar the Coso geothermal field (Southeastern California/USA) (Fig., 45).This model is available in the Kavaklıdere geothermal field.

Paper ID: ART2018930 DOI: 10.21275/ART2018930

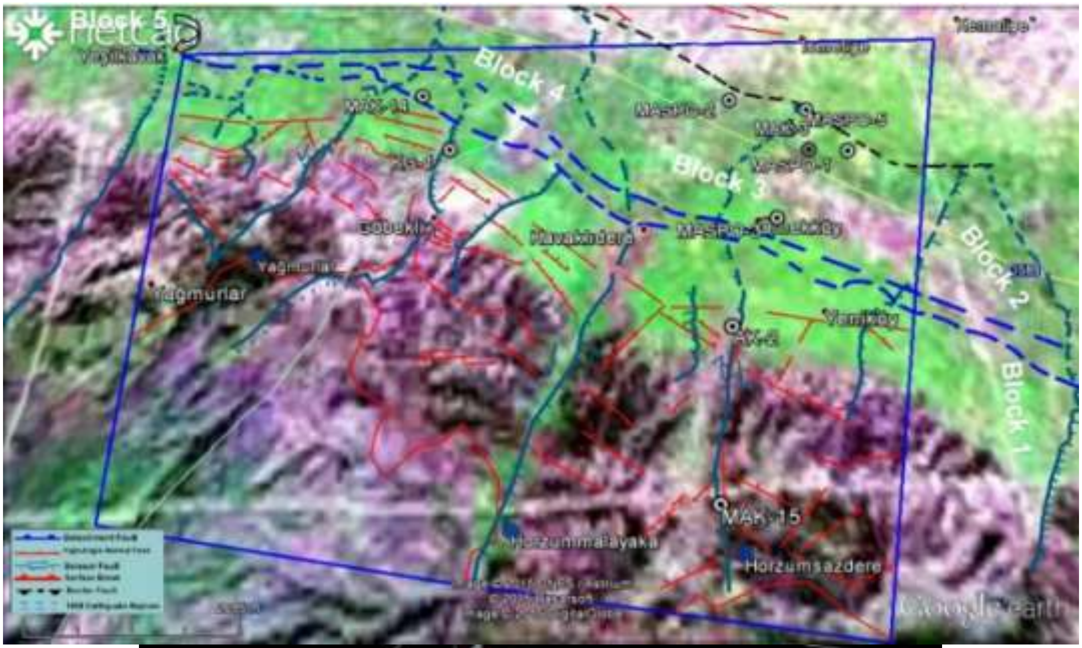

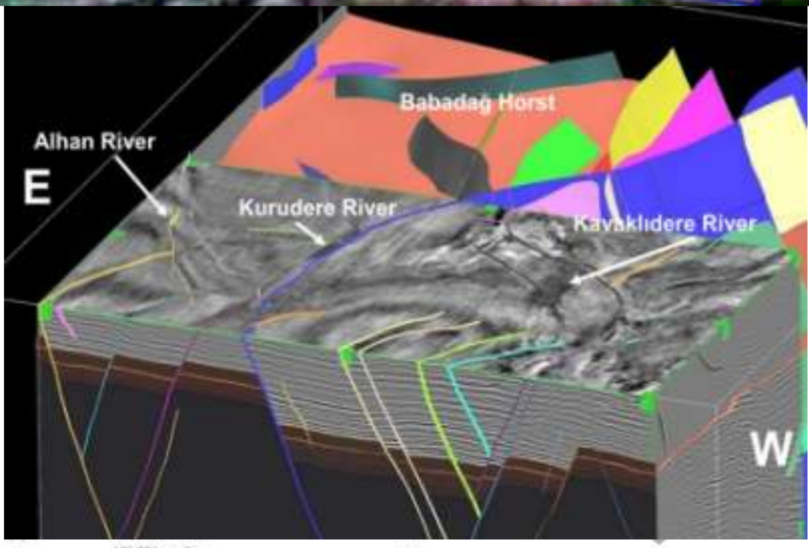

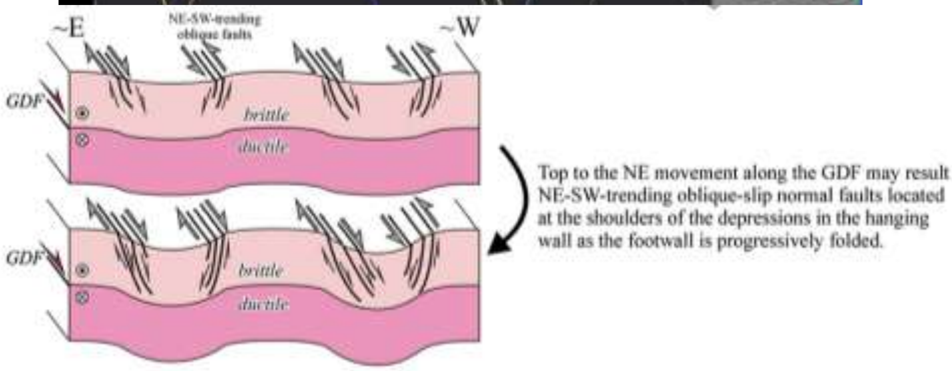

Figure 44: Potential geothermal reservoirs (Block 3 and Block 4) are detected at the result of the geophysical measurements and geological interpretations

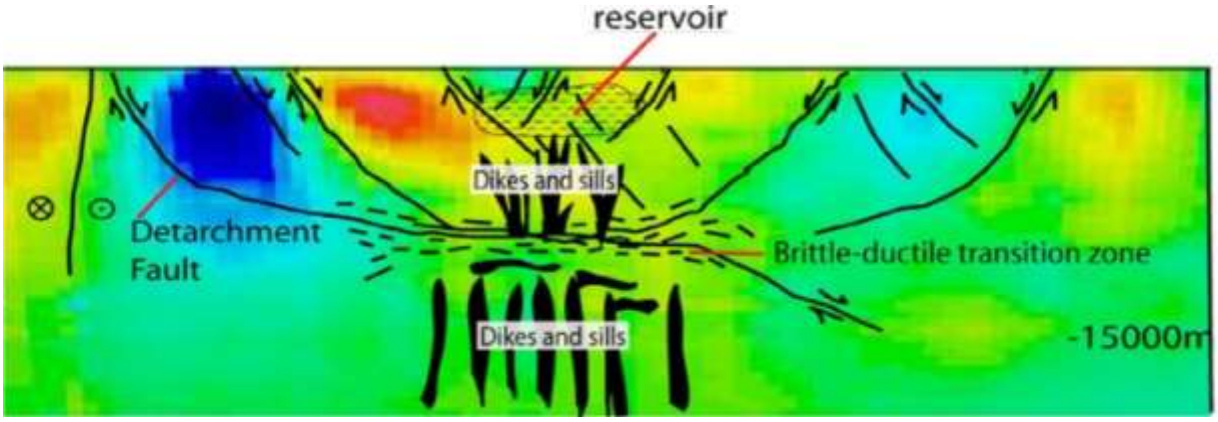

Figure 45: Summary of the geophysical and geological interpretation of the structures within the Kavaklıdere geothermal field (from Wamalwa et al., 2013)

3. Conclusions

The Kavaklıdere geothermal field which covers a 126 km^2 area between Alaşehir and Salihli districts in Manisa province, Turkey were studied. The geophysicfeatures connected to geological structure and the properties of geothermal systems in the field were measured. Various electrical resistivity and thermal methods in geothermal exploration were applied in the field. VES applications AB/2 = 2500 m theoretical depth in 206 locations were performed.In addition to total 206 resistivity measurements were compared with previous studies and all measurements were re-evaluated with EarthImager 1D and RockWorks programs. VES curves, resistivity and stratigraphy cross-sections were re-prepared and re-interpreted according to revealuating results.Potential geothermal reservoirs were detected at the result of the geophysical measurements made for determining the expected thermal activities at intersection points of the different orientioned faults mostly located at middle and north sides of the study area. By considering geologic and tectonic compability, it was expected to gather fluid with higher temperature and flow from the drillings going to be open.

The geothermal activities at the Kavaklıdere geothermal field appear to lie at the intersections of minor northerly striking sinistral normal transfer faults and the Gediz detachment fault. Left steps in the transfer faults at the intersection with the detachment were inferred to represent dilational jogs that provide channelways for geothermal fluids. The left steps may result from refraction across the detachment surface that results from the mechanical contrast between hanging-wall sedimentary rocks and basement gneisses, marbles, and schists in the footwall. Brecciated marble at these intersections was seen to provide good reservoirs for the geothermal fluids. The reservoirs was determined as plunging gently northward along the intersection of the detachment fault with the transfer faults. Although this model can account for the shallow reservoir and surface springs, it may not predict the location of the main upwelling that feeds these geothermal systems. Major steps in the Alaşehir frontal fault or complex fault intersections between the transverse faults and WNW-striking normal faults may accommodate upwelling in the Kavaklıdere geothermal field.

High resistivity zones were interpreted to be regions of cooled intrusions with minimum porosity and permeability. Unfractured rocks were marked by intermediate to high density zones and high resistivities. The locations of the reservoir region and dikes and sills that provide heating for the system were interpreted. These models were made to present an improved and more complete picture of the upper crustal structure of the Kavaklıdere geothermal fields by identifying all the features related to the geothermal system.

References

[1] Emre, T., 1996. Gediz grabeninin jeolojisi ve tektoniği (Geology and tectonics of the Gediz graben). Turk. J. Earth Sci., 5, 171-185.
[2] Gürsoy, T., 1981. Turgutlu-Alaşehir gravite jeotermal etüt raporu (Report on Turgutlu-Alaşehir Geothermal Gravity Survey). MTA Report No:6695 (Unpublished).
[3] Hersir, G.P. and Bjornsson, A., 1991. Geophysical Exploration for Geothermal Resources, Principles and Application. UNU Geothermal Training Programme Reykjavik, Iceland Report 15, 94 p.
[4] Koçyiğit, A. 2014. Active tectonic evaluation of Kavaklidere (Manisa) license areas. 52 p (Unpublished).
[5] MTA, 2010. Manisa ve civari jeotermal enerji aramalari jeofizik (gravite-manyetik) etüd raporu (Yıldırım, G.) (Unpublished).
[6] MTA, 2011a. Manisa Alaşehir jeotermal enerji sahası MAK-14 ve MAK-3 kuyularının özet değerlendirilmesi (Dünya, H.) (Unpublished).
[7] MTA, 2011b. Manisa Alaşehir jeotermal enerji sahasi MAK-15 jeotermal kuyu geliştirme ve bitirme test raporu (Dünya, H. ve Bilgiç, Ö.) (Unpublished).
[8] MTA, 2011c. Manisa Alaşehir jeotermal enerji sahasi MAK-14 jeotermal kuyusunun RCHP ile temizliği, asitleme-geliştirme ve bitirme test raporu (Dünya, H., Bilgiç, Ö. ve Akgun, B.) (Unpublished).
[9] Öner, Z. and Dilek, Y., 2011. Supradetachment basin evolution during continental extension: The Aegean province of western Anatolia, Turkey. Geological Society of America Bulletin 123, 2115-2141
[10] Öner, Z., 2012. Supradetachment basin tectonics and the exhumation history of the Menderes core complex, Western Anatolia, Turkey. Miami University, Thesis of Doctorate of Philosophy. 223 p.

[11] Özdemir, A., 2015.Report on New Subsurface Geological Model and New Geothermal Model of the Kavaklıdere Geothermal Fıeld (Alaşehir / Manisa / Turkey), Batı Anadolu Jeotermal A.Ş: 623 p. (Unpublished).

[12] Özdemir, A., Yaşar, E. and Çevik, G., 2017. An importance of the geological investigations in Kavaklıdere geothermal field (Turkey). Geomechanics and Geophysics for Geo-Energy and Geo-Resources, v. 3(1), p.29-49.

[13] Seyitoglu, G., Çemen, I., and Tekeli, O., 2000. Extensional folding in the Alaşehir (Gediz) graben, western Turkey: Journal of the Geological Society of London, v. 157, p. 1097-1100.

[14] Şimşek, Ş., 2012. Advisory report on geological-hydrogeological-geophysics and potential assessment evaluation of Manisa-Alaşehir-Kavaklıdere geothermal license areas and determination of the exploration / production / reinjection well locations. 272 p (Unpublished).

[15] Türk, S., 2014. Sesmic structure and tectonics of the Alaşehir-Gediz graben, western Turkey, Miami University, Master of Science Thesis. 42 p.

[16] Ünal, A. and Havur, E., 1971. Alaşehir-Salihli bölgesinin jeotermik enerji yönünden detay jeoloji etüdü. MTA Report No ; 4678 (Unpublished).

[17] Wamalwa, A.M., Mickus, K.L., Serpa, L,F. and Doser, D.I., 2013. A joint geophysical analysis of the Coso geothermal field, south-eastern California. Physics of the Earth and Planetary Interiors, 214, 25-34

[18] Yazman, M.K. and Iztan, H., 1990. Alaşehir'in (Manisa) jeolojisi ve petrol olanakları. TurkishPetroleum Exploration Group, Technical Report, 18 p (Unpublished).

[19] Yazman, M.K., Güven, A., Ermiş, Y., Yılmaz, M., Özdemir, İ., Akçay, Y., Gönülalan, U., Tekeli, Ö., Aydemir, V., Sayılı, A., Batı, Z., İztan, H. and Korucu, Ö., 1998. Alaşehir Grabeni'nin ve Alaşehir-1 prospektinin değerlendirme raporu. Turkish Petroleum Exploration Group,Technical Report, 142 p (Unpublished).

[20] Yılmazer, S., Pasvanoğlu, S. and Vural, S., 2010, the relation of geothermal resources with neotectonics in the Gediz Graben (West Anatolia, Turkey) and their hydrogeochemical analysis, world geothermal congress, 25-30 April 2010, Bali, Indonesia, 1151 -1161.